

REVIEW

Interface triboelectricity

Jing You¹ | Jiajia Shao^{2,3} | Yahua He^{1,4}  | Bobo Sun^{2,3} | Khay Wai See¹ |
Zhong Lin Wang^{2,3,5} | Xiaolin Wang^{1,4} 

¹Institute for Superconducting and Electronic Materials, Australian Institute for Innovative Materials, University of Wollongong, Wollongong, New South Wales, Australia

²Beijing Institute of Nanoenergy and Nanosystems, Chinese Academy of Sciences, Beijing, China

³School of Nanoscience and Technology, University of Chinese Academy of Sciences, Beijing, China

⁴ARC Centre of Excellence in Future Low-Energy Electronics Technologies, University of Wollongong, Wollongong, New South Wales, Australia

⁵Georgia Institute of Technology, Atlanta, Georgia, USA

Correspondence

Xiaolin Wang and Khay Wai See.
Email: xiaolin@uow.edu.au and
kwsee@uow.edu.au

Funding information

Australian Government Global Innovation Linkage Program, Grant/Award Number: GIL 73629; Center of Excellence in Future Low-Energy Electronics Technologies, Australian Research Council, Grant/Award Number: CE170100039; Fundamental Research Funds for the Central Universities, Grant/Award Number: E0E48957; China Postdoctoral Science Foundation, Grant/Award Number: 2019M660766; National Natural Science Foundation of China, Grant/Award Numbers: 51432005, 51702018, 62001031; National Key R & D Project from Minister of Science and Technology of China, Grant/Award Number: 2016YFA0202704; Australian Research Council; Australian Government

Abstract

The exploration of triboelectricity at the liquid–solid (L–S) interface has sparked significant interest due to its potential for sustainable energy harvesting and technological advancement. Motivated by the need for innovative energy solutions and the unique advantages offered by liquid-based environments, a comprehensive review of the fundamental concepts, mechanisms, and applications of liquid–solid triboelectric nanogenerators (TENGs) is provided. Three basic working modes of liquid–solid TENGs and the distinct properties and mechanisms of each model are discussed systematically. The physical fundamental of liquid–solid TENGs is further investigated, which includes “Wang Transition”, Wang’s Hybrid Electric Double Layer model, tribovoltaic effect, equivalent circuit model, and the mechanisms of liquid–solid contact electrification based on density functional theory. Understanding charge transfer and charge distribution at the liquid–solid interface is also crucial to confirm the underlying mechanisms of liquid–solid TENGs. Finally, a broad range of applications of liquid–solid TENGs are explored, emphasizing their potential in addressing energy challenges and complex interdisciplinary issues that link the disciplines of materials science, chemistry, physics, and even electrical engineering.

KEYWORDS

interface triboelectricity, liquid–solid triboelectric nanogenerators, Wang’s hybrid electric double layer (EDL) model

Jing You and Jiajia Shao are contributed equally to this work.

This is an open access article under the terms of the [Creative Commons Attribution](https://creativecommons.org/licenses/by/4.0/) License, which permits use, distribution and reproduction in any medium, provided the original work is properly cited.

© 2024 The Author(s). *EcoEnergy* published by John Wiley & Sons Australia, Ltd on behalf of China Chemical Safety Association.

1 | INTRODUCTION

Triboelectric nanogenerators (TENGs) have emerged as a promising technology for energy harvesting, converting mechanical energy into electrical energy through the triboelectric effect and electrostatic induction.^{1–5} The triboelectric effect refers to the phenomenon of charge transfer that occurs when two dissimilar/same materials come into contact. This effect has been extensively studied in solid–solid interfaces,^{6–9} where materials with different electron affinities and work functions interact to generate static electricity. The exploration of triboelectric effect at the solid–liquid interface, where one of the materials is in a liquid state, has gained significant attention in recent years. Unlike solid–solid TENGs, where electron transfer is the primary mechanism, solid–liquid interfaces involve complex charge transfer processes, including both electron and ion transfer. This presents unique opportunities and challenges for understanding and optimizing TENG performance. Liquid–solid TENGs offer unique advantages over their solid–solid counterparts, such as flexibility, adaptability, and the ability to harvest energy from various liquid-based environments. These characteristics make them particularly suitable for applications in fields such as biomechanics,^{10–15} environmental monitoring,^{16–18} wearable devices,^{19–22} human–machine interfaces,^{23–26} and so on. Moreover, the diverse chemical properties of liquids,^{27,28} such as polarity, viscosity, and ionic composition, provide additional opportunities to not only enhance the performance of liquid–solid TENGs but also introduce complexities in understanding charge transfer mechanisms. Despite these advantages, significant challenges remain in fully understanding the underlying mechanisms of charge transfer at solid–liquid interfaces. For instance, the interplay between surface modifications, liquid dynamics, and material properties is still not fully explored. In particular, the interaction between electron and ion transfer processes has not been comprehensively studied, leading to research gaps that hinder the full optimization of liquid–solid TENG systems. Furthermore, theoretical models such as the overlapped electron cloud and electric double-layer models require further refinement to capture the complexities of the solid–liquid interface.

In this review, we provide a comprehensive analysis of the current state of liquid–solid TENGs, focusing on the fundamentals and applications of solid–liquid interface triboelectricity, aiming to provide a comprehensive understanding of this field and highlight its potential for various technological advancements. We begin by defining the concept of solid–liquid interface triboelectricity and exploring the motivations behind the liquid–solid TENGs, including the need of sustainable energy harvesting, the

advantages of liquid-based environments, and the unique challenges associated with the liquid–solid interface. The subsequent section of this review tries to elucidate the fundamental working modes of liquid–solid TENGs: liquid–dielectric, liquid–semiconductor, and liquid–metal (Figure 1). Each mode has its distinct properties and mechanisms, which we will discuss in detail through relevant studies and experimental results. We will reveal the relevant physical fundamentals of liquid–solid TENGs, including “Wang Transition”, Wang’s Hybrid Electric Double Layer (EDL) model, tribovoltaic effect in solid–liquid interface, equivalent circuit model of solid–liquid TENGs, the mechanisms of liquid–solid contact electrification (CE) based on Density functional theory (DFT), as well as charge distribution at liquid–solid interfaces. Understanding the charge transfer and charge distribution at liquid–solid interfaces is also crucial to comprehend the underlying mechanism of liquid–solid TENGs. So, the theoretical and experimental investigations of charge distributions at the interface and their influences on device performance as well as energy harvesting efficiency will be discussed thoroughly. Furthermore, a broad range of applications enabled by liquid–solid TENGs have been presented in the paper: rolling as micro/nano-power source, self-powered sensor, scanning probe system, blue energy harvesting device, and so on.

The rapid development of liquid–solid TENGs and corresponding fields has motivated the proposal of the interface triboelectricity concept. Despite positive progress, this concept is facing many challenges and opportunities. We anticipate that a deeper understanding of the working models, physical basis, and the applications of liquid–solid TENGs will be a supplement and advancement to the existing research of interface triboelectricity.

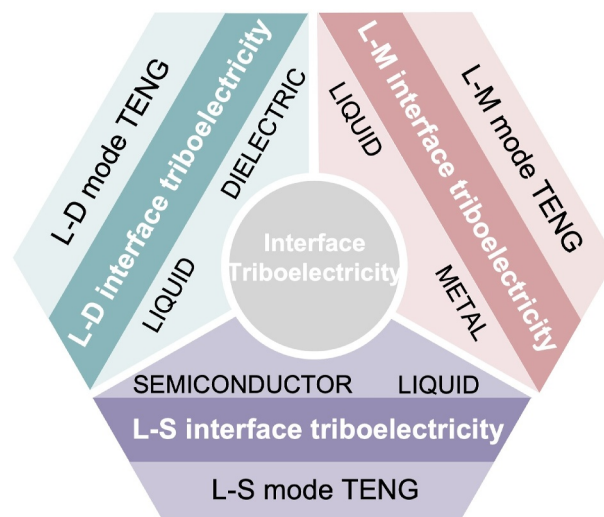


FIGURE 1 Schematic of the interface triboelectricity in three basic working modes of liquid–solid TENGs.

Through a comprehensive examination of the literature and important findings, we strive to shed light on the advancements made in this field and recognize the challenges and opportunities that lie ahead. It is our hope that this review would be served as a valuable resource for researchers, engineers, and professionals interested in the field of solid–liquid interface triboelectricity, inspiring further research and innovation in this evolving area.

2 | THREE FUNDAMENTAL WORKING MODES OF THE LIQUID–SOLID TENG

2.1 | Liquid-dielectric mode

The liquid-dielectric mode is one of the basic working modes in the realm of solid–liquid TENGs.^{2,29–32} In this mode, the liquid–dielectric interface is utilized to generate triboelectric charges and subsequently energy harvesting. The liquid employed in this mode serves as the medium for charge transfer and ion adsorption. When a dielectric material comes into contact with a liquid, generally, the electrons transferring from the liquid to the dielectric occurs due to the difference in electron affinity and electronegativity between the two materials, resulting in an electric potential difference across the interface. Upon separation, the electric potential difference increases and the corresponding current can be obtained if an external circuit is closed. Numerous studies have explored the liquid-dielectric mode and demonstrated its potential for efficient energy conversion.^{33–37} Various liquids have been investigated, which include water, organic solvents, and electrolytes.^{38,39} For example, You et al.⁴⁰ reported the use of water as the liquid medium in a liquid-dielectric TENG, where a multi-dielectric layer constructed from polyimide (Kapton) films and polytetrafluoroethylene (PTFE) films served as the dielectric material (Figure 2A). Figure 2B illustrates the modeled EDL formed on the water–solid interface, including the water–PTFE interface and water–electrode interface. The double layer is formed by a compact layer of charges next to the charged PTFE followed by a diffuse layer extending into bulk solution (DI water). The developed equivalent circuit model and governing equations for this water–solid mode TENG are presented in Figure 2C. Note that the equivalent model can be extended to other types of liquid–solid TENGs. Based on the first-order lumped circuit theory, the water–solid mode TENG is equivalent to a series connection of two EDL capacitors and a water resistor. By examining the output characteristics and critical influences of this model, they provided insights into the

physical mechanisms underlying the operation of the water–solid mode TENG.

Similarly, Zhao et al.³⁸ introduced a self-powered, long-lasting, and highly selective oil–solid TENG (O-TENG) for energy harvesting and intelligent monitoring (Figure 2D–E). The O-TENG formed by the dielectric materials exhibits excellent electrical output performances and shows exceptional sensitivity and remarkable durability, presenting a promising approach for enhancing the output and durability in oil–solid contact, enabling intelligent energy harvesting and oil condition monitoring. Nie et al.³⁶ conducted a comprehensive investigation to elucidate the mechanism of CE between a liquid triboelectric layer and a solid material. Their study focused on the triboelectrification process between PTFE and various solvents, such as water, NaCl, and CuSO₄. Figure 2F demonstrates the method for testing the amount of charges on a water droplet after liquid–solid (L–S) friction. Extrusion of water droplets with two PTFE films coated on fluorine-doped tin oxide glass increases the L–S contacting area and charge transfer. Their findings revealed that the charge transfer between water and PTFE primarily involved electron transfer, while ion transfer played a dominant role in the ionic liquid–solid interface (e.g., NaCl–PTFE). Increasing the concentration of ions in the solution is beneficial for the charge transfer. Notably, irrespective of the type of ions, the amount of charge generation between the ionic liquids and PTFE exhibits a similar pattern. In addition, Zou et al.^{41,42} introduced a universal method to quantify the triboelectric series for various polymers (Figure 2G). Through the measurement of dielectric materials with a liquid metal under well-defined conditions, they derived a normalized triboelectric charge density to reveal the intrinsic character of polymers in terms of gaining or losing electrons. This quantitative triboelectric series serves as a textbook standard, facilitating the application of triboelectrification in energy harvesting and self-powered sensors. More importantly, their research clarifies the charge polarity and magnitude in liquid–solid interfaces, which is extremely helpful for reasonable design and optimization of liquid-dielectric TENGs.

Furthermore, Lin et al.⁴³ conducted a study focusing on quantifying electron transfer during the liquid–solid CE and investigating the formation of electric double-layer simultaneously (Figure 2H). They examined the CE at the liquid–solid interface and studied the decay of charges on solid surfaces under different thermal conditions. To differentiate the contribution of electron transfer from that of ion transfer on the charged surfaces, they applied the theory of electron thermionic emission. It is revealed that both electron transfer and ion transfer occur in the liquid–solid CE. Then, the researchers

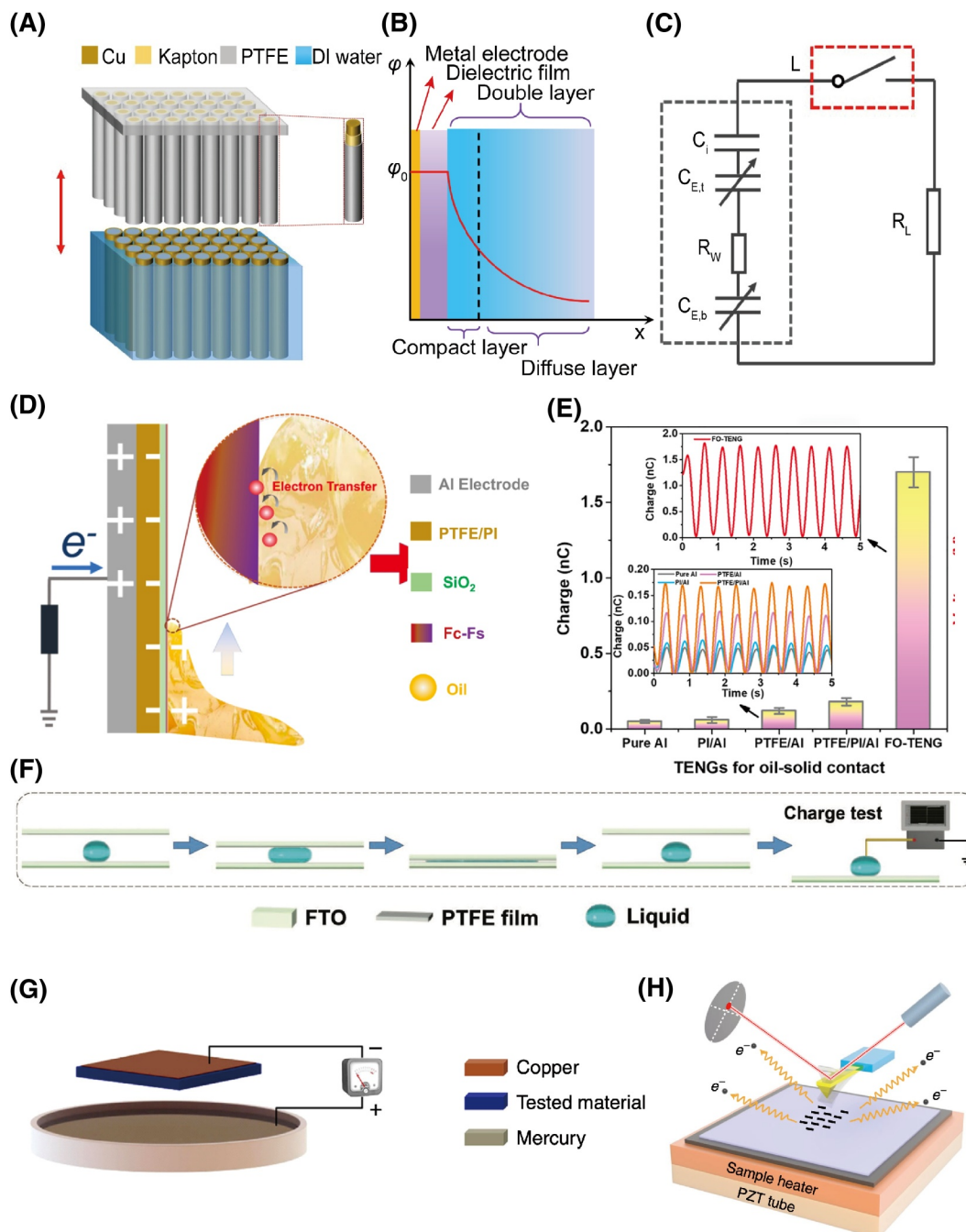


FIGURE 2 Typical liquid-dielectric mode TENG. (A) Schematic diagram of the three-dimensional water–solid TENG array. (B) Typical electrical double layer formed on the water–dielectric interface area and the relevant variation of electrostatic potential φ with distance x from the electrode, and (C) the full equivalent circuit model of the water–solid triboelectric nanogenerator. (D) Schematic illustration of the triboelectric mechanism of the FO-TENG (where an O-TENG modified with different amounts of Fc(x) and Fs(y) is denoted as FO-TENG(x - y)) and (E) transferred charge curves of the FO-TENG compared with other O-TENGs for oil–solid contact. (F) Method for testing the amount of charge on a water droplet after L–S friction. (G) Simplified model of the measurement method. The tested material contacts the liquid metal mercury and then separates periodically. The positive electrode of the electric meter is connected to the mercury, and the negative electrode is connected to the copper electrode. (H) The setup of an atomic force microscope (AFM) platform for the thermionic emission experiments.

proposed a two-step model encompassing electron and/or ion transfer to successfully demonstrate the formation of an EDL in the process of liquid–solid CE. Moreover, to

improve the performance of the liquid-dielectric mode TENG, researchers have adopted different methods to try to solve this problem. For instance, structured surfaces

such as micro/nanostructured patterns or porous materials^{44–47} can effectively increase the contact area, thus facilitating more efficient charge transfer. Additionally, the introduction of functional coatings or surface modifications^{48–53} on the dielectric material can enhance the triboelectric charging process either.

2.2 | Liquid-semiconductor mode

The liquid–semiconductor mode is another basic working modes in the realm of solid–liquid TENGs. In this mode, the interface between a liquid and a semiconductor material is utilized to create triboelectric charges and subsequently energy harvesting. The generation of charges at the liquid–semiconductor interface is due to the tribovoltaic effect. The physical basis of the tribovoltaic effect results from the electron–hole pairs generating at the p – n junction because of the energy released by the formation of newly formed chemical bonds at the interface.^{42,54} These electron–hole pairs, also known as excess carriers, are driven to drift or diffuse within the space charge region by two forces: the diffuse force created by carrier density gradients; and the built-in electric field, which acts in the opposite direction. Liquid–solid CE based on the tribovoltaic effect will be further discussed in chapter 3.2.

Several studies have explored the liquid–semiconductor mode TENGs and demonstrated their potential for efficient energy conversion.^{55–57} Lin et al.⁵⁸ designed experiments to investigate the tribovoltaic effect occurring at an interface between an aqueous–silicon interface. A syringe conductive needle was used to drag a DI water droplet sliding over a silicon wafer surface (Figure 3A), and the tribo-current and tribo-voltage were observed (Figure 3B,D). It is found that a direct current (DC) tribo-current was generated during the sliding process, as shown in Figure 3D. The direction of the tribo-current was from p/n -type silicon to the aqueous solution in the external circuit. Combining I – V characterizations, the direction of the tribo-current at the sliding aqueous–silicon interface is the same as the direction of the built-in electric field at the interface, which was consistent with the tribovoltaic effect. In the field of tribovoltaic effect research, the impact of temperature on the liquid–solid interface has been studied by Zheng et al.⁵⁹ Their studies investigated the relationship between the temperature and the tribo-voltage/current at interfaces such as water/Si and water/metal during sliding (Figure 3E). Their findings revealed that increasing the temperature resulted in higher tribo-voltage/current outputs (Figure 3F). Furthermore, the researchers demonstrated the synergistic effect of the liquid's pH value and temperature on the tribovoltaic

effect. To explain the observed phenomena, an energy band model was proposed (Figure 3C), which highlights the role of “bindington” energy—energy released through the formation of chemical bonds between the liquid and solid—during the tribovoltaic effect. The significant results shed light on the intricate interplay between the temperature, the pH value, and the tribovoltaic effect at the liquid–solid interface, which is helpful to understand the working mechanism of liquid–semiconductor mode TENG and its applications in energy harvesting or self-powered sensors.

2.3 | Liquid-metal mode

Liquid–metal mode is another interface type that has been explored in recent years. For instance, Le et al.⁶⁰ provided theoretical insights into the vibrational spectra of metal–water interfaces using density functional theory-based molecular dynamics (DFTMD). Figure 4A illustrates the structure of the Pt⁶¹–water interface at the potential of zero charge from DFTMD trajectory. The isosurfaces show the electron density difference profile of the interface before and after electronic interaction between the water and metal surface. The cyan and yellow regions signify electron depletion and accumulation, respectively. Within the model, water molecules are categorized as watA, watB, and watC (Pt, watA, watB, and watC are colored in gray, blue, magenta, and red, respectively.) based on their distance from the metal surfaces. WatA molecules, closest to the surfaces (Pt and Au), chemisorb via their oxygen atoms with dipoles pointing outward, resulting in partial electron transfer to the metal surfaces. WatB molecules, slightly above watA within the adsorption water layer, interact weakly with the metal surfaces, exhibiting no preferred adsorption site and negligible charge transfer to the metal. WatC molecules fall outside the water adsorption layer, lacking direct interaction with the metal surfaces and serving as the “bulk” reference. The study includes calculations of the vibrational density of states for watA, watB, and watC at the Pt⁶¹– and Au⁶¹–water interfaces, respectively. Calculation results indicate that the specific adsorption of surface water on Pt⁶¹ leads to partial charge transfer to the metal and strong hydrogen bonding with neighboring water molecules. Although their study was focused on the vibrational properties, it contributes to our understanding of the interface behavior between metals and liquids, which is crucial for elucidating the charge transfer mechanism and optimizing the performance of liquid–metal mode TENG.

In addition, another study by Quang et al.⁶² presented a direct-current fluid-flow-based TENG (DC–FluTENG),

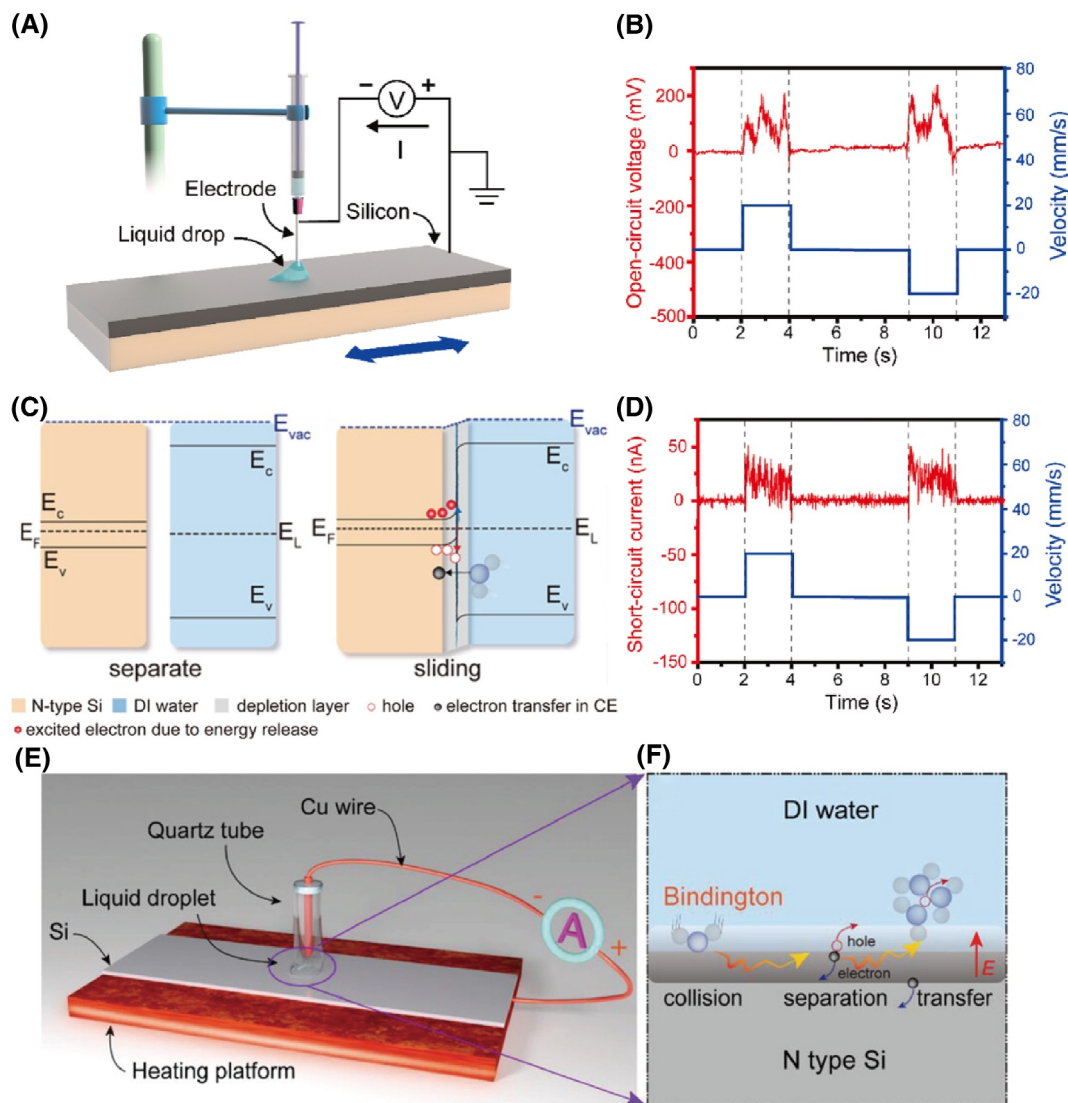


FIGURE 3 Typical liquid-semiconductor mode TENG. (A) The setup of the tribovoltaic experiment and the external circuit, (B) oscillogram of the open-circuit voltage when a DI water droplet slides on a *p*-type silicon wafer (0.1 Ω cm) at 20 mm/s, and the droplet static contact diameter is 2.5 mm, (C) energy band diagram of *n*-type Si and DI water, (D) oscillogram of a short-circuit current when a DI water droplet slides over a *p*-type silicon wafer (0.1 Ω cm) at 20 mm/s, and the droplet static contact diameter is 2.5 mm, (E) the setup of the experiments, and (F) a schematic diagram of the generation of tribocurrent.

which offers a simple but effective mechanical-to-electrical energy conversion technology for harvesting hydrokinetic energy. The DC-FluTENG was experimentally measured using the setup depicted in Figure 4B. The experimental apparatus includes a microprocessor-controlled tubing pump employed to induce the flow of water droplets within the system. The fabrication of the DC-FluTENG cell is simple with a pin-type electrode positioned near the pipe's end and connected to the ground, thereby establishing a single-electrode mode of operation. Note that its geometry structure is different from a conventional single-electrode mode TENG. The experimental results showed an open-circuit voltage of 35 V, a short-circuit current of 3.7 μ A, and a peak power

of 57.6 μ W, respectively (Figure 4C). The study also investigated other important influences such as water droplet type, flow rate, and electrode material, which can extremely affect the output performance of the direct-current fluid-flow-based TENG.

The liquid-metal mode offers unique advantages due to the excellent electrical conductivity of the metal. This enables efficient charge transfer and low-resistance pathways for the current flow, leading to improve energy harvesting capabilities. Additionally, the selection of appropriate metal materials and the optimization of their surface properties^{52,63,64} can further enhance the output performance of liquid-metal mode TENGs. Further research and optimization of this mode will contribute to

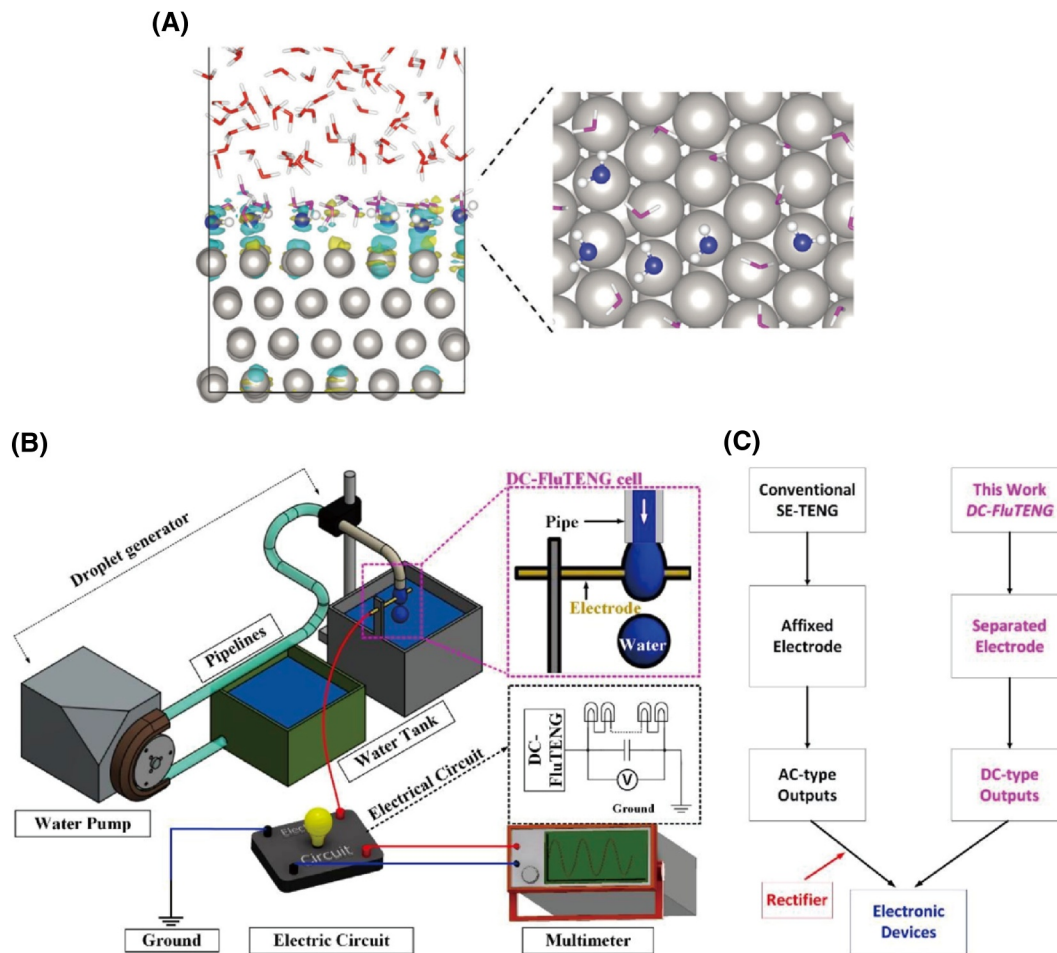


FIGURE 4 Typical liquid-metal mode TENG. (A) Side (left) and top (right) views of a snapshot of the Pt⁶¹-water interface from a density functional theory-based molecular dynamics (DFTMD) trajectory. Pt, watA, watB, and watC are colored in gray, blue, magenta, and red, respectively. (B) Schematic illustration showing the experimental setup of a DC-FluTENG and (C) structure diagram of the DC-FluTENG in comparison with a conventional single-electrode-based TENG. DC, direct current.

the development of practical applications in micro/nano-power sources, self-powered sensors, and other emerging fields.

3 | PHYSICAL FUNDAMENTALS OF LIQUID-SOLID TENG

3.1 | “Wang transition” for CE and Wang’s hybrid EDL model

CE at the liquid-solid interface is a complex phenomenon that plays a major role in the operation of solid-liquid mode TENGs. Traditionally, CE has been extensively studied in solid-solid interfaces,⁶⁵ where charge transfer occurs between two solid materials upon contact and separation. The introduction of liquids into the CE process, however, introduces additional complexities due to the presence of ions and the formation of EDLs.⁶⁶

Understanding the dynamic processes for CE and formation of EDL is essential for optimizing the performance of liquid-solid TENGs. The “Wang transition” and Wang’s hybrid EDL model^{67,68} expatiate valuable insights for these processes, which clarify the mechanisms at the liquid-solid interface.

The “Wang Transition” is a concept introduced to explain electron transfer during liquid-solid CE, which is a fundamental process in triboelectric nanogenerators (TENGs). In classical models, charge transfer was mainly attributed to ion transfer, but recent studies have highlighted the role of electron transfer as a critical mechanism. The “Wang Transition” specifically addresses the scenario where two materials, A and B, come into close contact as depicted in Figure 5.⁵⁴ Normally, without contact, electrons in material A remain confined due to the significant potential barrier separating the two materials, preventing electron transfer. However, when intimate contact is made, the electron clouds of atoms in

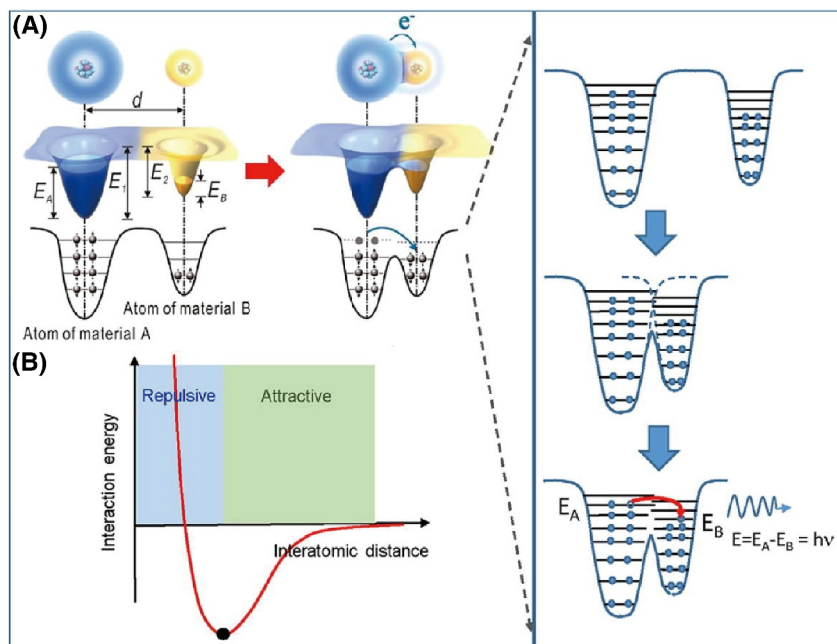


FIGURE 5 (A) An electron-cloud-potential-well model proposed for explaining contact electrification (CE) and charge transfer. d , distance between two nuclei; E_A and E_B , occupied energy levels of electrons; E_1 and E_2 , potential energies for electrons to escape. (B) Interatomic interaction potential between two atoms when they are at the equilibrium position.

materials A and B overlap, reducing the potential barrier. This allows electrons to move from material A to lower energy levels in material B, completing the “Wang Transition”. During this transfer, the electrons may also release photons as they transition to lower energy states, a phenomenon observed experimentally.

The electron transfer process should not be ignored during the CE and the formation of EDL. The classical EDL model, which focuses primarily on the ionized interaction at the liquid–solid interface, has proven insufficient to explain the complete charge dynamics observed in systems like liquid–solid TENGs. Wang’s hybrid layer, first proposed by Wang et al. in 2018,⁶⁹ introduces a “two-step” mechanism that incorporates both electron transfer and ion adsorption, providing a more comprehensive explanation of the interfacial charge behavior. Initially, liquid molecules and ions engage the solid surface because of thermal activity and liquid pressure. The overlapped electron clouds between solid atoms and water molecules facilitate electrons exchange. Traditional EDL models suggest that the ionized interaction on the liquid–solid interface induces more charges on the surface, leading to charge distribution and compensation in the diffusion layer. In the hybrid layer, the charge transfer between solid and liquid molecules causes even more charges to be accumulated at the surface. This electron transfer process works parallel to the ion adsorption process.

Lin et al.⁴² studied the CE between liquids and solids and investigated the decay of CE charges on the solid surfaces under different thermal conditions (Figure 6C–D). The contribution of electron transfer is distinguished from that of ion transfer on the charged surfaces by using the electron thermionic emission theory. The experiments show that there are both electron transfer and ion transfer in liquid–solid CE. This is the first time that the “two-step” model for the formation of the EDL, in which the electron transfer plays a dominant role, has been verified experimentally. The “Wang transition” and Wang’s hybrid EDL model serve as critical tools for investigating and comprehending the complex charge transfer mechanism and the behavior of EDL in liquid–solid CE.

3.2 | Liquid–solid CE based on tribovoltaic effect

The tribovoltaic effect is a new concept that describes the generation of an electric potential difference upon contact and separation involving semiconductors.^{70–72} The mechanism of the tribovoltaic effect is resulted from the electron-hole pairs generated at the P - N junction due to the energy released by the formation of the newly formed chemical bond at the interface due to mechanical sliding. This section explores the fundamental principle and

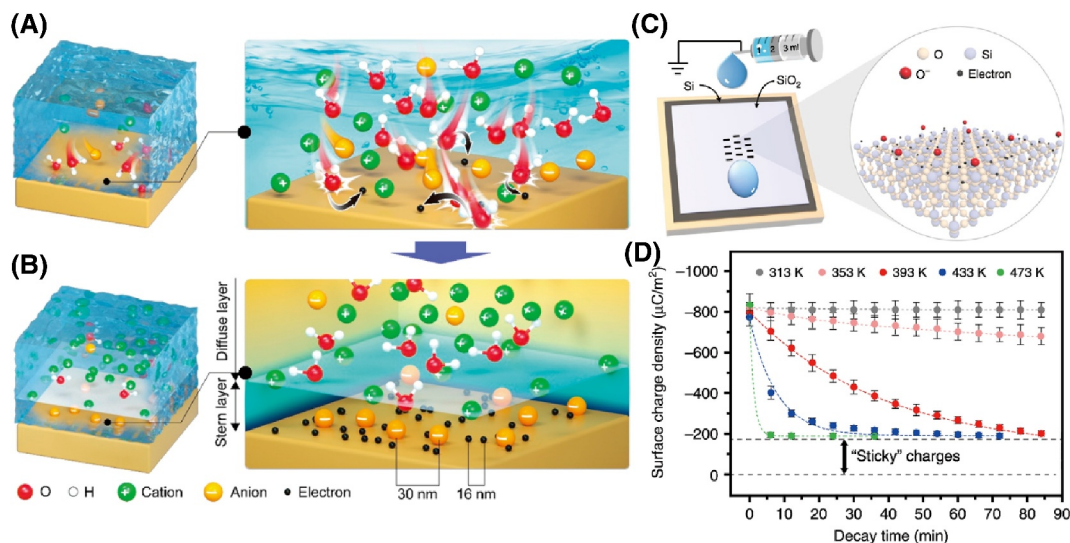


FIGURE 6 (A)–(B) Wang's hybrid Electric Double Layer (EDL) model and the “two-step” process for its formation. (A) In the first step, the molecules and ions in the liquid impact on the solid surface due to their thermal motion and the pressure from the liquid, which leads to electron transfer between them; meanwhile, ions may also attach themselves to the solid surface. (B) In the second step, free ions in the liquid would be attracted to the electrified surface due to electrostatic interactions, forming an EDL. (C) The setup of the charging experiments, where the negative charges generated on the SiO₂ surface, could be electrons and O[−] ions induced by the surface ionization reaction. (“O” is the oxygen atom, “Si” is the silicon atom, and “O[−]” is the oxygen ion). (D) The decay of the contact electrification (CE) charge (induced by contact with the DI water at room temperature) on the SiO₂ surface at different substrate temperatures.

mechanism underlying the liquid–solid CE based on the tribovoltaic effect. The tribovoltaic effect governs CE in the context of semiconductors in which electron-hole pairs are excited at the *P-N* junction or the Schottky junction during friction. The excited electrons are further driven by the built-in electric field to move from one side to the other side at the interfaces, generating a direct current. This effect is similar to that of the photovoltaic effect, with the mainly difference being that the electron-hole pairs in the triboelectric effect are excited by the “bindington” rather than light irradiation. The tribovoltaic effect in liquid–solid CE is influenced by various factors, including the materials, surface properties, the nature of the liquid medium, and so on. Researchers have extensively investigated this effect to understand its mechanism and optimize its performance in TENG applications.^{73–75}

Zhang and Wang's group in their study⁷⁶ were the first to demonstrate the presence of the tribovoltaic effect between metal and solid surfaces. They introduced a metal-semiconductor direct-current triboelectric nanogenerator (MSDC-TENG) built on the principle of the tribovoltaic effect (Figure 7A). This effect is enhanced by the direct voltage and current generated when a metal/semiconductor is rubbed against another semiconductor. The thus-formed atomic bonds release frictional energy, exciting nonequilibrium carriers, which, are separated directionally to form a current. When the metal and

silicon slide against each other, the MSDC-TENG consistently exhibits an open-circuit voltage (10–20 mV) (Figure 7B), a short-circuit direct-current output (10–20 μA) (Figure 7C), and a low impedance characteristic (0.55–5 kΩ). The researchers conducted a systematically study of these working parameters to understand their effects on electrical output and impedance characteristics. The groundbreaking work not only broadens the scope of material candidates for TENGs but also provides a fresh perspective on an electric energy conversion mechanism based on the tribovoltaic effect.

Furthermore, a study conducted by Lin et al.⁵⁸ explored the tribovoltaic effect at the liquid-semiconductor interface. This research involved generating both tribo-voltage and tribo-current by moving a droplet of DI water across silicon surfaces with varied doping types and concentrations. The analysis of voltage-current measurements indicated that there is a built-in electric field at the interface between DI water and silicon. The directions of both the tribo-voltage and tribo-current are found to be dependent on the built-in electric field, suggesting that the tribo-voltage and tribo-current are induced by the tribovoltaic effect. Consequently, it is inferred that the energy released from electron transfer, when the liquid contacts the silicon, stimulates the electron-hole pairs at the silicon surface. Driven by the built-in electric field at the liquid–solid junction, the electron and hole are separated, finally

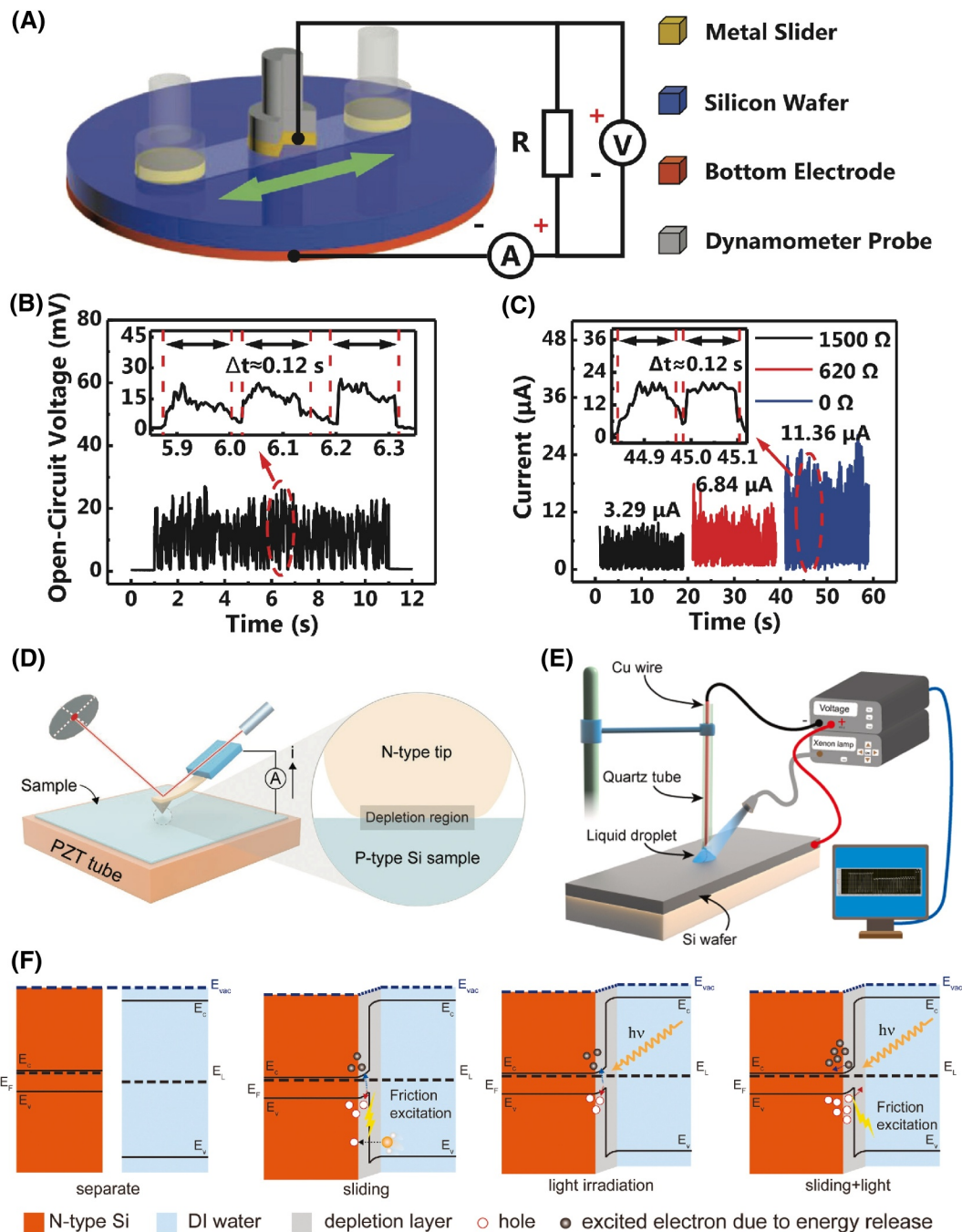


FIGURE 7 Liquid–solid contact electrification (CE) based on the tribovoltaic effect. (A) Schematic illustration of a metal–semiconductor-based direct current TENG (MSDC-TENG). (B)–(C) The electric output characteristics of the MSDC-TENG. (D) The setup of the conductive atomic force microscopy experiment platform, with the diamond coated tip controlled to rub on the Si sample with a certain load. During the rubbing, the current between the tip and the sample was recorded using a conductive atomic force microscope (CAFM). (E) The setup of the experiments showing the coupling of the photovoltaic effect and the tribovoltaic effect at the DI water and Si wafer interface under light irradiation and (F) energy band diagram of the interaction between the *n*-type Si and the DI water.

generating the observed tribo-voltage and tribo-current. This study marks a significant milestone in our understanding, as it is the first experimental verification of the tribovoltaic effect at a liquid–solid interface.

Building on this body of research, a study by Zheng et al.⁷⁷ provided microscopic evidence supporting the

existence of the tribovoltaic effect. They successfully generated a direct current by sliding an *N*-type diamond coated tip over Si samples with various doping concentrations (Figure 7D). They study discovered that the tribo-current between the Si samples escalated in line with an increase in both the density of the surface state of the Si

sample and the sliding load. This observation turns out that the tribo-current between two semiconductors (or a semiconductor and a metal) is induced by the tribovoltaic effect. The findings suggest that at the interface, the energy released due to the transition of electrons from the surface states of one semiconductor to the other, and also from bond formation across the sliding interface, could potentially excite electron-hole pairs. Besides, the separation of electron-hole pairs by the built-in electric field at the *P-N*, *N-N*, and Schottky junction may induce the observed current. This is the first time the tribovoltaic effect has been clearly explained and validated at a microscopic level. These findings also propose a novel method for enhancing the output current in electric generators based on the tribovoltaic effect.

In a groundbreaking study in 2021, Wang's group⁷⁸ formulated the first explanation of the fundamental physical mechanism of the tribovoltaic effect. This study centered on generating tribo-voltage and tribo-current at the DI water-semiconductor interface under light irradiation (Figure 7E). The research revealed that the directions of the tribo-current and photo-current were congruent and both of them are dependent on the built-in electric field at the DI water-semiconductor interface. Significantly, it was found that light irradiation can amplify the tribo-current, with the enhanced tribo-current intensifying proportionately to the light intensity and inversely to the light wavelength. This supports a hypothesis that the tribo-current was instigated by the tribovoltaic effect. In this process, the electron-hole pairs at the interface are excited by the "bindington" and mobilized by the built-in electric field at the heterojunction. Furthermore, the researchers proposed an energy band model (Figure 7F) to explicate the interaction between the tribovoltaic and photovoltaic effects. In this model, the enhancement of the tribovoltaic current is attributed to the increased concentration of electron-hole pairs under light irradiation. These studies, among others, highlight the pivotal role of the tribovoltaic effect in liquid-solid CE within the realm of TENGs.

3.3 | Equivalent circuit model of liquid-solid TENG

The development of equivalent circuit models has proven to be a valuable approach for analyzing the electrical behavior of TENGs.⁷⁹⁻⁸² The equivalent circuit models of liquid-solid TENGs typically include components such as resistors, capacitors, and current or voltage sources. Utilizing equivalent circuit models, researchers can gain insights into the basic mechanisms governing the electrical behavior of liquid-solid TENGs. The theoretical

works proposed by Niu et al.,⁸³⁻⁸⁷ Jiang et al.,⁸⁸ and Shao et al.⁸⁰ provide a solid foundation for developing these models specifically for liquid-solid TENGs. In general, TENGs are categorized into five distinct operational modes based on their geometry structure and mechanism works. These encompass the contact-mode TENGs, sliding-mode TENGs, single-electrode TENGs, free-standing TENGs, and rotary-mode TENGs. Each operational mode of the TENG has its own output characteristics. Through the process of CE, electrostatic charges are engendered and subsequently distributed on the contacting surface. As there is a positional shift of the dielectric, alterations in the potential difference instigate electron transfer between the metal electrodes to try to keep electrostatic equilibrium. These theoretical works serve as a basis^{89,90} for constructing equivalent circuit models for TENGs with different configurations, including those operating on the liquid-solid interface.

Xu et al.⁹¹ proposed a droplet-based electricity generator (DEG) based on the finding that continuous impinging water droplets on a fluorinated material lead to a high charge density on its surface. The DEG device, illustrated in Figure 8A, is constructed by the drop-casting polytetrafluoroethylene (PTFE) combined with a small aluminum fragment onto a glass substrate pre-coated with indium tin oxide (ITO). When a water droplet impinges and spreads on the device, it bridges the previously separated components, resulting in a closed-loop electrical system. In the associated circuit model, the expanding droplet acts as a resistor, while the PTFE functions as a capacitor, C_P , with the water/PTFE representing the top plate and PTFE/ITO the bottom plate. In the switched-off state, no capacitor emerges at the water/aluminum juncture, thereby keeping C_P and C_I in an open circuit, preventing charge flow (see Figure 8B). Conversely, in the switched-on state, the connection of the aluminum electrode and PTFE by the water droplet results in the creation of an additional capacitor, C_2 , at the water/aluminum boundary, converting the previously open circuit into a closed one. Within the circuit, R_w , R_L , and $dq(t)/dt$ in the circuit are the impedance of the water droplet, the impedance of the external load, and the time derivative of the transferred charge, respectively. This circuit model effectively predicts the DEG device's output characteristics, aligning with experimental findings.

Wu et al.⁹² developed a quantitative model of the electrical response caused by the impact of a drop onto an electrical nanogenerator (ENG) surface, as depicted in Figure 8C. They deployed millimeter-sized droplets from a specific height onto surfaces that were either horizontal or slightly inclined. These surfaces were coated with an amorphous fluoropolymer (AFP), specifically Teflon. Prior to experimentation, these polymer films were

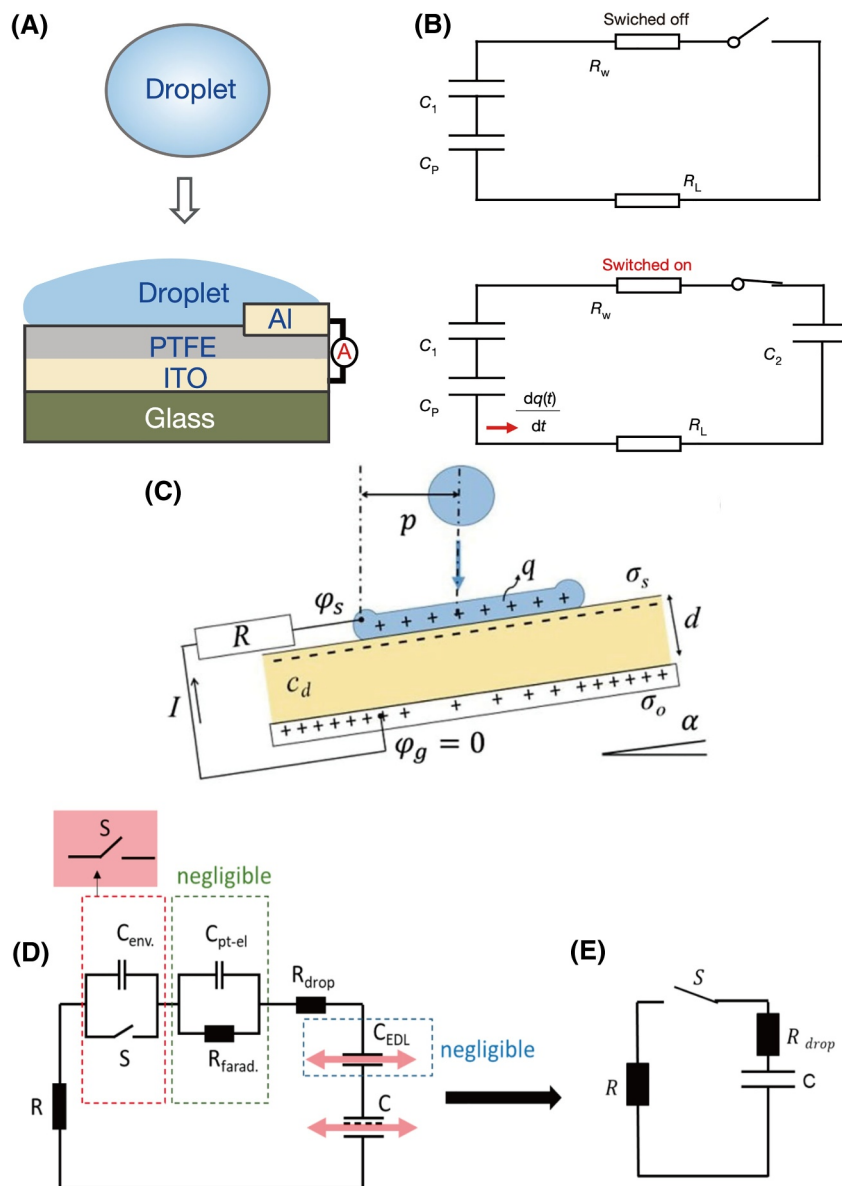


FIGURE 8 Equivalent circuit model of liquid–solid TENG. (A) Schematic diagram of droplet-based electricity generator (DEG) and (B) circuit model. In the switched-off mode, there is no capacitor formed at the water/aluminum interface. As a result, C_p and C_1 remain in an open circuit and there is no charge flow between them. When the aluminum electrode and PTFE are connected by the water droplet (switched-on mode), another capacitor, C_2 , is established at the water/aluminum interface, forming a closed circuit. R_w , R_L , and $dq(t)/dt$ in the circuit are, respectively, the impedance of the water droplet, the impedance of the external load, and the derivative of the transferred charge with respect to time. (C) Experimental setup, (D) full equivalent circuit, and (E) simplified equivalent circuit of the water drop electricity generator.

electrically charged. An electrode on the substrate is connected to a thin Pt wire, positioned parallel to the substrate via an external load resistor R . The comprehensive equivalent circuit of the water drop electricity generator is presented in Figure 8D. Here, C_{env} represents the capacitance from the environment before the water droplet contacts the wire. Given $C_{env} \rightarrow 0$, it can be considered as an open circuit. Hence, the section of Figure 8D involving C_{env} can be substituted by a switch,

S , in the simplified circuit. Upon the droplet's contact with the Pt wire, a faradaic impedance forms at the Pt electrode/electrolyte interfaces. Considering the double layer capacitance is considerably larger than the dielectric capacitance and the overall circuit's capacitance is calculated as $C = (\sum 1/C_i)^{-1}$, the EDL capacitance at the electrode/electrolyte C_i interface, C_{pt-el} , becomes negligible. Similarly, the EDL capacitance at the dielectric/electrolyte interface, C_{EDL} , is also negligible within the

circuit. As a result, the circuit is simplified as displayed in Figure 8E. It can be concluded that these models, when properly constructed and utilized, provide a powerful tool for analysis, optimization, and design of liquid–solid TENG systems.

3.4 | Mechanisms of liquid–solid CE based on the DFT

Understanding the mechanism of CE at the liquid–solid interface is essential for revealing the fundamental processes involved in TENGs. DFT has emerged as a powerful tool to investigate the mechanism of CE at the atomic and molecular levels.^{93,94} Wu et al.⁹⁵ conducted an atomic-level investigation on the effect of CE on the liquid–solid EDL, utilizing first-principle and molecular dynamic simulations. This study revealed that liquid–solid CE affects the concentration distribution of molecules and ions in the EDL. Additionally, it can reverse the polarity of the double layer, depending on the specific surface charge density. The proposed mechanism is illustrated in Figure 9. When the SiO₂ surface is negatively charged, the electric field generated by these negative charges synergistically amplifies with the inherent local polarized electric field. This mutual enhancement results in a strengthening of the EDL (Figure 9A). Conversely, if the SiO₂ surface is positively charged, the electric field generated by these positive charges counteracts its intrinsic local polarized electric field. This opposition leads to a restraint or even a reversal of the EDL (Figure 9B). It is mainly contributed to a fact that the surface charge density on the solid surface can substantially affect the adsorption energy between the anion/cation and the solid surface (Figure 9C). These findings not only support Wang's two-step model but also offer a more detailed understanding of how liquid–solid CE influences the formation of the EDL.

Nan et al.⁹⁶ employed DFT to study CE at the water/polymer interface. In their work, some representative polymers containing different functional groups and repeat units are selected (Figure 9D). Various factors have been considered in the study, including the influence of the water layer, molecular chain length, contact modes, electrostatic potential, and work function before and after CE. The theoretical results highlight that electron transfer predominantly occurs at the water/polymer interface when the two materials come into contact with each other. Moreover, only the outermost layer of the water has a significant contribution. The highest occupied molecular orbital (HOMO) and lowest unoccupied molecular orbital (LUMO) gap states on the surface act as electron acceptors, and notably, a wider HOMO-LUMO gap enhances electron transfer efficiency. Nan's

research clarifies the complex mechanisms underlying CE, offering profound insights into the dynamics of charge transfer and distribution at the liquid–solid interface.

Using DFT to study liquid–solid CE has also facilitated the exploration of the influence of environmental factors, such as temperature and humidity.^{97–100} By considering the vibrational and electronic properties of the materials, DFT calculations have provided insights into the temperature-dependent charge transfer and the influence of moisture on the CE behavior. Furthermore, DFT simulations have enabled the exploration of the impact of surface modifications, such as coatings or functionalization on the CE process.^{49,101–103} By considering electronic structures, interfacial interactions, and environmental factors, DFT simulations have enhanced our understanding of charge transfer processes, EDL formation, and the influence of surface modifications.

3.5 | Charge states at the liquid–solid interface

Understanding charge states at the liquid–solid interface is important to comprehend the intricate processes involved in CE and the operation of liquid–solid TENGs. The charge distribution and polarization effects at the interface play a significant role in determining the generation and transfer of electrical charges.^{90,104–108} As electrons and ions accumulate at the interface, they form localized electric fields, which in turn influence the further transfer of charges. Polarization effects, resulting from differences in material properties, can enhance or hinder charge mobility, ultimately affecting the efficiency of charge separation and transfer during the CE process. Studies have shown that these interfacial fields can even reverse charge polarity depending on the conditions of contact and surface chemistry. In this section, we investigate the charge states at the liquid–solid interface and their impact on the CE phenomenon.

The study of liquid–solid TENGs and charge states at liquid–solid interfaces has attracted much attention recently. Shin et al.¹⁰⁹ introduced a theoretical triboelectric series based on the thermoelectric effect, providing a foundational work for understanding charge transfer systems in triboelectric nanogenerators. Furthermore, liquid–solid triboelectric probes are developed for the real-time monitoring of charges at the liquid–solid interface, demonstrating the potential of improving detection capabilities.¹¹⁰ Moreover, the role of electrostatic charges in regulating chemiluminescence at the liquid–solid interface has been explored, highlighting the importance of understanding charge carriers,

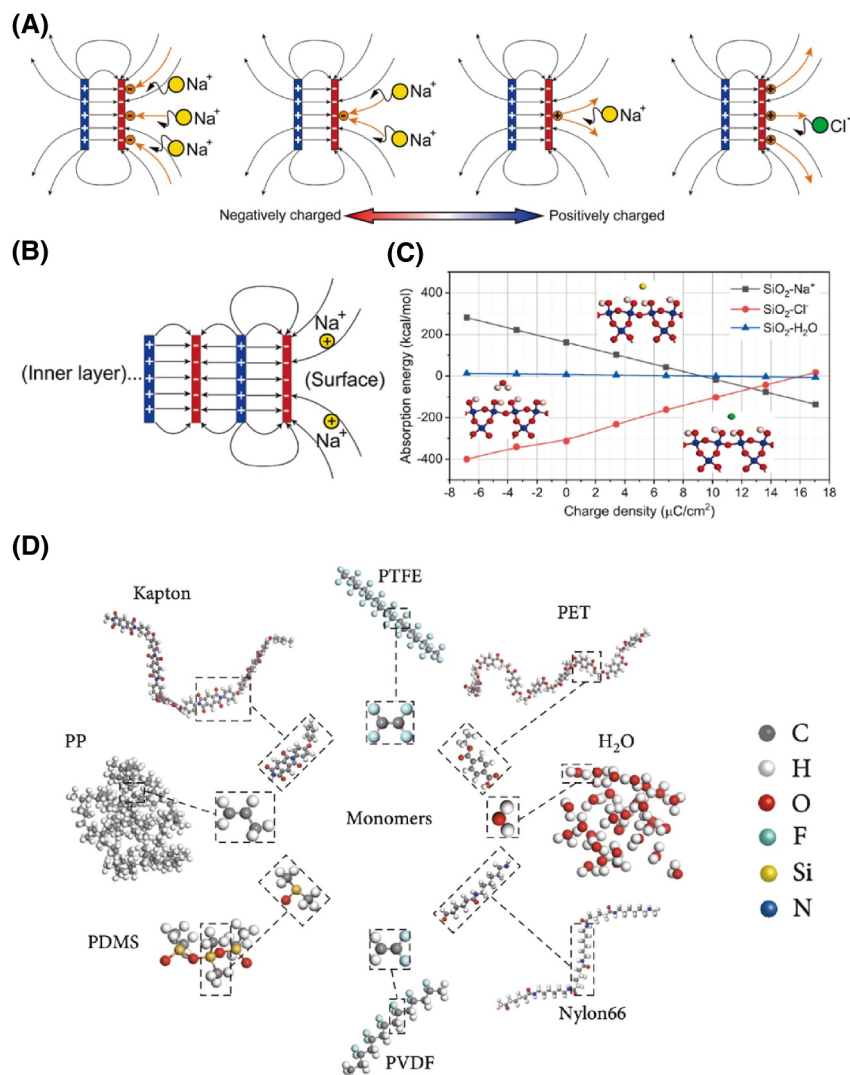


FIGURE 9 (A) Diagrams of the mechanism influencing the surface charge density on the formation of an Electric Double Layer (EDL), with the solid surface charged very negatively, less negatively, less positively, and very positively. (B) Analysis of the local polarized electric field on an SiO₂ surface. (C) The adsorption energy between an SiO₂ surface and an Na⁺ ion, Cl⁻ ion, and H₂O molecule under different charge densities. (D) Structures of seven polymers. Polytetrafluoroethylene (PTFE), polypropylene (PP), polyvinylidene difluoride (PVDF), polydimethylsiloxane (PDMS), Nylon 66, polyimide (Kapton), polyethylene terephthalate (PET), and water. The dashed areas depict their monomers.

particularly electrons in triboelectricity.⁶¹ This research stresses the multifaceted nature of charge interaction at the interface and their potential implications for diverse technological applications. Moreover, a liquid–solid interface-based triboelectric tactile sensor was developed, showcasing the potential for utilizing charge states to enhance sensor performance.¹¹¹ This innovation underscores the versatility and potential of manipulating charge states for improving sensing capabilities and expanding its applicability of triboelectric technologies.

The various models discussed—Wang Transition, hybrid electric double-layer (EDL) model, tribovoltaic effect, equivalent circuit model, and DFT—can be

synthesized into a unified framework to comprehensively explain the charge transfer processes in liquid–solid TENGs. Initially, the Wang Transition and EDL model describe the interaction between electrons and ions at the liquid–solid interface, where CE begins as the liquid meets the solid. The tribovoltaic effect complements this by explaining the electron transfer during continuous frictional contact. These microscopic processes are captured in the equivalent circuit model, which represents the macroscopic electrical behavior of the TENG, linking the internal charge dynamics to the measurable output of the device. Meanwhile, DFT calculations provide a quantum mechanical perspective on electron

behavior at the atomic level, offering deeper insights into the charge transfer mechanisms and material interactions. Ultimately, the charge states at the liquid–solid interface integrate these models by describing how charge is distributed and stabilized, considering external factors such as temperature. Together, these models provide a holistic understanding of the charge generation, accumulation, and retention processes, forming a foundation for optimizing TENG performance.

4 | APPLICATIONS OF LIQUID–SOLID TENG

4.1 | As micro/nano-power sources

One of the remarkable applications of liquid–solid TENGs lies in their potential as micro/nano-power sources. The ability to convert mechanical energy into electrical energy at small scales opens up a wide range of possibilities for self-sustained power generation in various microelectronic and nanoscale devices. Micro/nano-power sources based on liquid–solid TENGs offer several advantages over traditional energy harvesting technologies. They can harness ambient mechanical energy sources, such as vibrations, human motion, or fluid flow,^{112–116} to generate electricity, thereby providing a sustainable and self-powered solution. Besides, liquid–solid TENGs exhibit a compact and lightweight design, making them highly suitable for integration into miniaturized electronic devices and wearable technologies.^{19,21,22,117–121} In this section, we explore the applications of liquid–solid TENGs as micro/nano-power sources and their remarkable contributions to the field.

Tang et al.¹²² introduced a self-powered water splitting system by integrating a TENG with a water splitting unit (Figure 10A–C). When the assembled TENG operated at a rotating speed of 600 rpm, the system yielded hydrogen at a rate of $6.25 \times 10^{-3} \text{ ml min}^{-1}$ with a 30% (w.t.) potassium hydroxide solution. Interestingly, when the electrolyte was swapped out for pure water, the water splitting efficiency increases by 4–5 times compared to water splitting powered by an electrochemical workstation, primarily because of the TENG's high voltage output. Moreover, a TENG can be powered by a flow of regular tap water, illustrating its capability as a truly self-sustaining water splitting system. Consequently, TENG-driven water splitting has emerged as a viable method for in situ hydrogen production, whether for energy storage or chemical reactions, without the need of an external power source.

Zou and colleagues¹²³ reported a bionic stretchable nanogenerator (BSNG) designed for underwater energy

harvesting that was inspired by the structure of ion channels found in the electrocyte cytomembrane of electric eels (*Electrophorus electricus*). To replicate this structure, a mechanical control channel was created using the stress-mismatch between polydimethylsiloxane (PDMS) and silicone (Figure 10D). The BSNG allows two different working modes, achieving an open-circuit voltage of over 170 V in dry conditions and more than 10 V (Figure 10F) in a liquid environment. This performance is enhanced by combining the benefits of the TENG, positioning the BSNG as a versatile tool for energy harvesting and underwater sensing. Combining the triboelectrification effects from flowing liquid with principles of electrostatic induction, practical underwater applications of this bionic stretchable nanogenerator were also demonstrated, including monitoring human motion in different positions and facilitating undersea rescue systems. With its exceptional flexibility, stretchability, impressive tensile fatigue resistance (surpassing 50 000 cycles), and superior underwater functionality, the bionic stretchable nanogenerator stands out as a promising sustainable power source for soft wearable electronics.

In fact, liquid–solid TENGs offer tremendous potential as micro/nano-power sources, enabling self-sustained energy harvesting for various microelectronic and nanoscale devices.^{124–126} Their compact design, ability to harness ambient mechanical energy, and integration capabilities with other technologies make them highly attractive for applications in water splitting, underwater sensing, and beyond. Continued research and development in this area will further unlock the possibilities of liquid–solid TENGs, leading to advances in self-powered micro/nano-systems and contributing to the field of sustainable energy harvesting.

4.2 | As self-powered sensors

Self-powered sensors based on liquid–solid TENGs can autonomously generate electrical power from mechanical energy sources in their surrounding environment, eliminating the need for external power supplies or batteries. This kind of new sensors offer several advantages over conventional sensors. They provide a sustainable and independent power source, enabling continuous and reliable operation without the need for frequent battery replacements or wired connections. The special feature is particularly advantageous for fluid energy harvesting, where battery life and power availability are critical factors. In this section, we explore the application of liquid–solid TENGs as self-powered sensors and their contributions to the field.

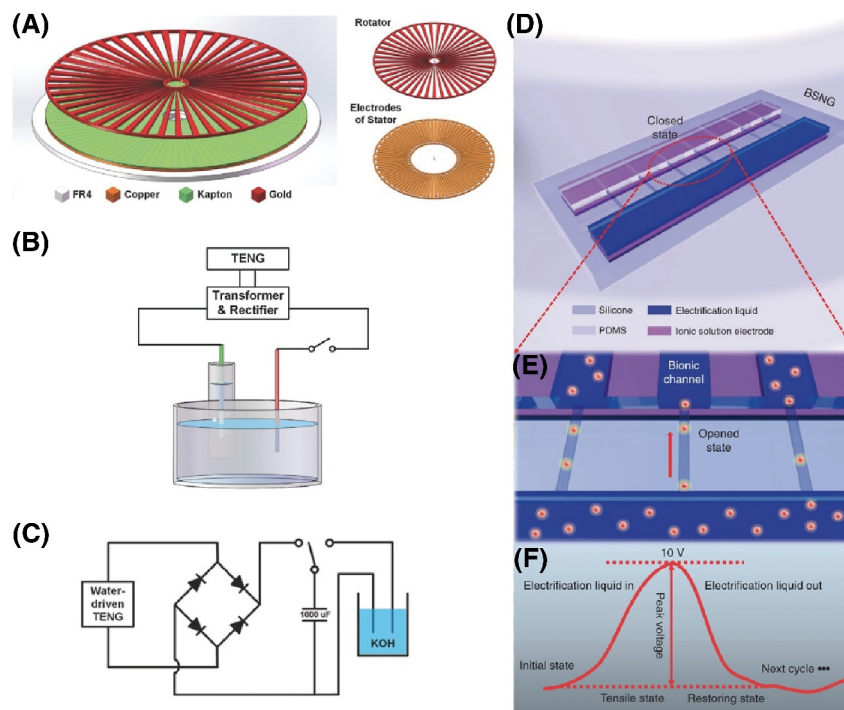


FIGURE 10 (A) Schematic illustration of the disk TENG, (B) schematic diagram, and (C) the circuit diagram of the TENG-driven water splitting system. (D) Schematic illustration of the bionic stretchable nanogenerator (BSNG) with double layer structure, which is mainly constructed from silicone, polydimethylsiloxane (PDMS), electrification liquid, and the ionic solution electrode. (E) Schematic diagram of the bionic channels in BSNG. (F) Output signal of BSNG in one working cycle.

Song's group¹²⁷ reported a water wave motion sensor (Figure 11A) based on water wave friction. By merging both the mechanisms of the outermost interface friction with water waves and the traditional TENG functionality, the sensor can detect enhancements in water waves at mild frequencies in typical living environments. Through systematic testing under various water levels and frequencies, the team observed and analyzed voltage and current signals. These signals could reach up to approximately 60 V and 20 μ A (Figure 11B–C), respectively, during specific surging wave conditions. Notably, the device can register even minor changes in water levels, clearly visualizing waveform variations. It is anticipated that this technology will showcase virtual advances in environmental monitoring, as well as maritime security and navigation.

Fluid energy includes a range of sources from large-scale ones such as wave energy to water flow energy, which are frequently found in rivers and pipelines.¹²⁸ A novel water wheel-based hybrid TENG has been developed by Wang's group.¹²⁹ It combines a water-TENG and a disk-TENG to simultaneously harvest both electrostatic and mechanical energy from flowing water (Figure 11D). The water-TENG features wheel blades coated with superhydrophobic surfaces, which are further covered by PTFE thin films with nanostructures. This design enables

the designed TENG to harvest electrostatic energy from the water. On the other hand, the disk-TENG consists of two disks. One of these disks rotates in tandem with the wheel blades when impacted by flowing water, functioning as a rotating disk mode TENG to harvest the water's mechanical energy. Notice that the short-circuit current of the disk-TENG is directly proportional to both the rate of flowing water and the wind speed (Figure 11E–F). This characteristic highlights the hybrid TENG's potential as a self-powered sensor for measuring both water flow and wind speed. The hybridized TENG provides a novel approach to harvesting multiple types of energy from the environment. Similarly, the Liquid-Piston-based Triboelectric Nanogenerator (LP-TENG) showcases the effective use of pipe mechanisms to generate electrical power from the dynamic movement of fluids through its structure.¹³⁰ By leveraging the direct interaction between the fluid and the tube's inner surface, where the triboelectric effect from their contact and separation produces electrical energy, LP-TENG exemplifies innovation in harnessing fluid dynamics for autonomous monitoring, particularly useful in remote or inaccessible locations, making it an ideal candidate for sustainable and efficient real-time fluid monitoring.

In addition to wave energy and water flow energy, droplet energy acts as an important source of liquid

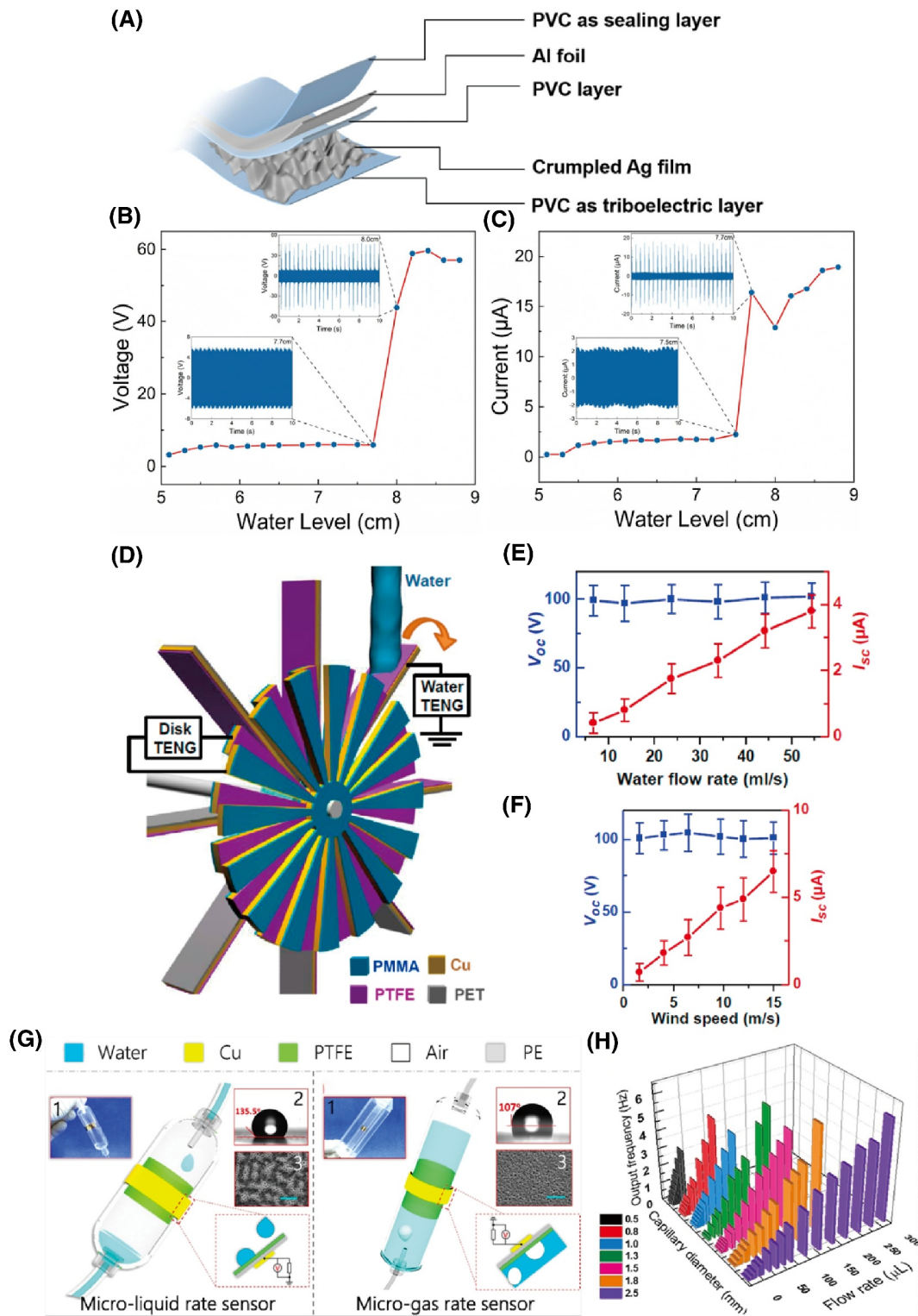


FIGURE 11 (A) Structure of the water-wave motion sensor rooted in water-wave friction, (B) peak values of voltage, and (C) peak values of current for the device. (D) Schematic illustration of the structure of the hybridized TENG. (E) The dependences of the open-circuit voltage (V_{oc}) and short-circuit current (I_{sc}) values on the flowing water rate of the disk-TENG. (F) The dependences of V_{oc} and I_{sc} values on the wind speed of the disk-TENG when it is driven by wind. (G) Schematic illustrations of the liquid rate sensor and gas rate sensor. For the liquid rate sensor, inset 1 shows a photograph of the sensor fabricated on a medical infusion tube, inset 2 shows the surface scanning electron microscope (SEM) image of the PTFE layer (scale bar: 5 μm), and inset 3 shows the contact angle, which indicates the hydrophobic property of the PTFE surface. For the gas flow rate sensor, inset 1 shows a photograph of the sensor fabricated on a pressure equalization (PE) tube, inset 2 shows a surface SEM image of the PTFE layer (scale bar: 3 μm), and inset 3 shows the contact angle of the air bubble on the PTFE surface. (H) 3D graph shows the output frequency of a self-powered triboelectric microfluidic sensor (TMS) with various capillaries under different external flow rates.

sensing. Leveraging droplet energy sensing, Chen et al.¹³¹ designed a self-powered triboelectric microfluidic sensor (TMS). This sensor capitalizes on the signals generated from droplets or bubbles through capillary actions and the triboelectrification effects at the liquid/solid interface, enabling real-time liquid and gas flow detection (Figure 11G). Through alternating capillaries of different diameters, both the sensor's detection range and sensitivity can be adjusted (Figure 11H). Evidence from monitoring the transfusion process for a patient and observing the gas flow from an injector indicates that the TMS offers significant potential for crafting a self-powered total microanalysis system.

Self-powered sensors based on liquid–solid TENGs offer tremendous potential for a wide range of applications. Their ability to harvest mechanical energy and convert it into electrical power enables continuous and autonomous sensing without the need of external power supplies or batteries. These sensors can find applications in environmental monitoring, health monitoring, smart grids, and environmental energy harvesting,^{132–136} providing reliable, sustainable, and self-powered solutions. The advances in liquid–solid TENG technology will further enhance the capabilities of self-powered sensors, contributing to the development of the innovative and autonomous sensing system.

4.3 | As scanning probe

The capability to measure charge transfer at the liquid–solid interface holds promise for a range of scientific applications. TENGs have emerged as pivotal tools in this field, not only as energy harvesters but also as insightful probes for charge transfer dynamics. Zhang et al.¹³⁷ pioneered in this field with the development of a droplet-TENG, distinguished by its dual spatially arranged electrodes (Figure 12A). This design aimed to systematically investigate the charge transfer dynamics between the liquid droplet and the solid substrate. Their findings revealed an intriguing accumulation of charges during droplet interaction, with electrons emerging as the main charge–transfer agents. It should be noticed that the sensitivity of the droplet-TENG to varying solvent ratios in mixed organic solutions paves the way for potential chemical sensing applications.

The same group unveiled the intricacies of charge transfer during the movement of a water droplet on hydrophobic surfaces.¹³⁸ This was achieved through the introduction of a high-density electrode array, termed the pixelated droplet-TENG. This setup enabled a detailed visualization of charge transfer at the liquid–solid boundary (Figure 12B). One important outcome was the

generation of an “image” illustrating the transferred charges with remarkable spatial and temporal fidelity. The study revealed a nonuniform distribution of charges along the droplet's pathway, suggesting a two-step mechanism involving electron transfer and subsequent ion adsorption on the solid interface, leading to the formation of an EDL. Such rigorous investigations underscore the profound probing capabilities of TENGs. Utilizing the ability of charge transfer at the liquid–solid interface, the potential applications of liquid–solid TENGs could extend across the following fields, such as surface chemistry, physics, materials science, and cell biology.^{139–143}

4.4 | Other applications

Apart from their utilization in micro/nano-power source, self-powered sensor, and scanning probe, liquid–solid TENGs have demonstrated potential for other different applications. Blue energy stands out as one of the most promising sources of renewable energy for expansive applications. In this context, liquid–solid TENGs have been proven effective in harnessing large-scale blue energy. Li and colleagues²⁹ developed a liquid–solid-contact (LS) buoy TENG specifically to harvest blue energy from the ocean (Figure 13A–B). This network of buoy LS TENGs can tap into vast energy reserves, capturing both surface wave energy and submarine current energy. Such harvested energy can power portable electric devices or navigation systems. Remarkably, in their study, the electrical energy generated from the LS TENGs was stored in capacitors, driving a wireless SOS (Save Our Souls) radio frequency transmitter for marine emergencies. Their research not only offers a more efficient way to tap into blue energy but also broadens its potential applications.

Furthermore, liquid–solid TENGs can be utilized in water and wastewater treatment systems to address energy challenges and enhance overall efficiency. By harvesting the flowing kinetic energy of water with a rotating TENG (R-TENG), Chen et al.¹⁴⁴ demonstrated a self-powered multi-functional system (Figure 13C–D). This system is capable of electrochemically eliminating rhodamine B (RhB) and copper ions from wastewater while simultaneously achieving metal electrodeposition. Their work demonstrates a sustainable approach to wastewater treatment, offering several advantages: high efficiency in removing RhB and copper ions, suitability for low-concentration organic pollutants, extremely low cost, simplicity, and reusability. This approach not only enables environmentally-friendly wastewater treatment, but also supports self-powered electrochemical process marked by minimal power use and pollution.

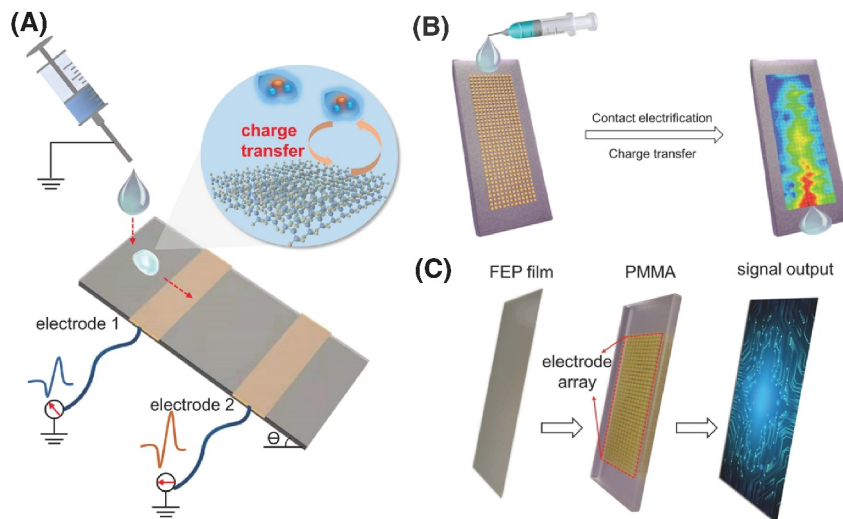


FIGURE 12 TENGs as scanning probes. (A) Working mechanism of the droplet-TENG. When a drop of liquid flows through the polymer surface, the charge transfer between the liquid and the solid occurs, and the current signals are separately measured by the two Cu electrodes. (B) Working mechanism of the pixelated droplet-TENG. When a water droplet flows through the tilted fluorinated ethylene propylene surface, the charge transfer between the liquid and the solid occurs, and the induced charges at each point are measured by the electrode arrays on the back side. (C) Structure of the pixelated droplet-TENG: the top layer is a dielectric polymer fluorinated ethylene propylene film (FEP film) for contact electrification (CE) with water droplets; the middle layer is a poly(methyl methacrylate) (PMMA) plate, with the Cu electrode array (12×36 Cu electrodes) penetrating the PMMA plate; and the bottom layer is a signal processor.

The electrowetting technique is a special method which can manipulate the position and velocity of fluids within microchannels. By integrating the electrowetting technique with a free-standing mode TENG, Nie et al.¹⁴⁵ designed a self-powered microfluidic transport system (Figure 13E). In this setup, a mini vehicle is fabricated by using four droplets to carry a pallet, and, driven by a TENG, it can transport a tiny object on the track electrodes under the drive of TENG. The motion of the TENG can provide both driving power and control signal for the mini vehicle. Using this TENG, the minimum volume of the droplet can reach 70–80 nL, while the tiny droplet can freely move on both horizontal and vertical planes. The team also illustrated a technique to transport nanoparticles to specified positions. Such an innovative self-powered transportation mechanism holds promise for micro-solid/liquid manipulation, drug delivery systems, micro-robotics, and human–machine interfaces.^{145–155} Figure 14 presents an overview of the principal applications emerging from Wang’s hybrid EDL two-step model and its associated fields. These applications cover a range of fields including bioelectronics, electric engineering, marine environmental monitoring, materials science, and other related disciplines. The figure provides a visual representation of how the theoretical insights from Wang’s model are translated into real-world applications, highlighting the broad scope and potential impact of the research in this field.

5 | CONCLUSIONS AND PERSPECTIVES

5.1 | Conclusions

The exploration of solid–liquid interface triboelectricity could open up new horizons in the field of energy harvesting and diverse technological applications. In this review paper, a comprehensive overview of the fundamental concepts, working modes, physical fundamentals, mechanisms, and applications of liquid–solid triboelectric nanogenerators (TENGs) are provided. We began by discussing the motivations behind the exploration of liquid–solid mode TENGs, highlighting the need for sustainable energy harvesting and the unique advantages offered by liquid-based environments. Then, three basic working modes of liquid–solid TENGs, the liquid–dielectric mode, the liquid–semiconductor mode, and the liquid–metal mode, are comprehensively investigated. Each mode presented distinct properties and mechanisms, allowing for versatile energy harvesting capabilities. The physical basis of solid–liquid interface triboelectricity is believed to be the “Wang Transition” and Wang’s Hybrid EDL model. These concepts provide a theoretical understanding of the charge transfer process and the formation of EDL at the liquid–solid interface. Furthermore, the mechanisms of liquid–solid CE are also explored through DFT, which clearly illustrates the underlying principles governing the charge transfer phenomenon.

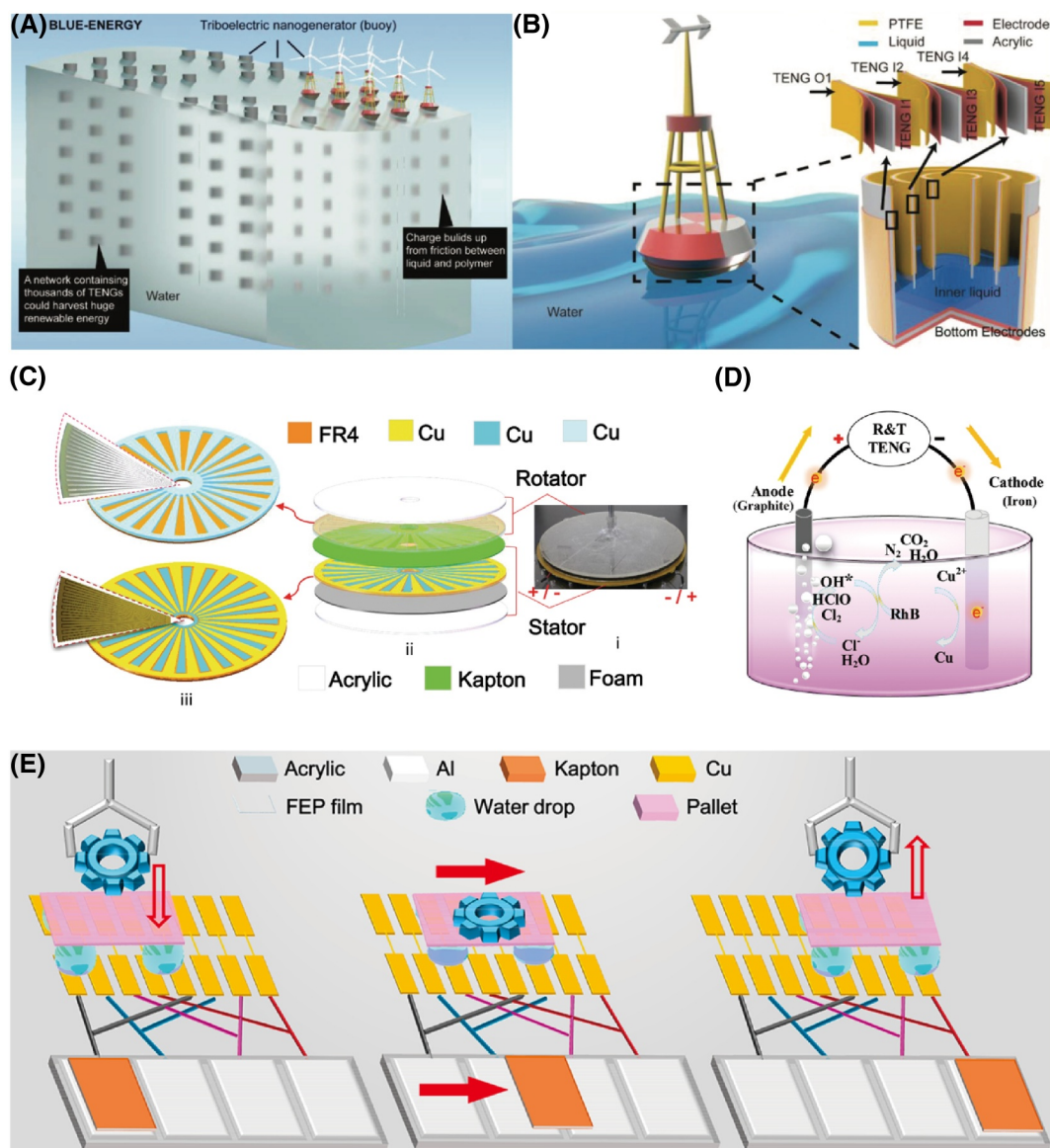


FIGURE 13 (A) Blue energy harvested by a network of liquid–solid-contact buoy triboelectric nanogenerators. (B) The structure of a buoy: the buoy contains an inner liquid and several polymer films, which function as several TENGs. (C) Schematic illustration of the R-TENG: (i) optical image and (ii) schematic exploded view of the R-TENG which consists of a rotator and a stator. (iii) Printed circuit board (PCB) patterns of the rotator and stator; insets are sectional optical images of PCBs. (D) Schematic diagram of the Cu²⁺ and rhodamine B (RhB) removal powered by a transformed and rectified TENG (R&T TENG). (E) Structure of the self-powered microfluidic transport system based on a TENG and the electrowetting technique to control the mini vehicle carrying a tiny gear.

By employing advanced characterization techniques and theoretical models, researchers have made significant progress in unraveling the intricacies of the charge state at the liquid–solid interface, paving the way for further improvement of liquid–solid TENGs. Additionally, the broad range of applications enabled by liquid–solid TENGs is discussed. These applications encompassed the micro/nano-power sources, self-powered sensors, scanning probe systems, and other emerging fields such as blue energy harvesting, wastewater treatment, and the electrowetting techniques. In a way, the exploration of solid–liquid interface triboelectricity could provide a new paradigm

for energy harvesting and diverse applications. The unique characteristics of liquid-based environments, coupled with the advances of understanding the charge transfer mechanisms, have laid a solid foundation for the development of efficient and versatile liquid–solid TENGs.

5.2 | Perspectives

Although interface triboelectricity is a relatively new and rapidly developing field, there remains considerable potential for discovery and optimization. To guide future

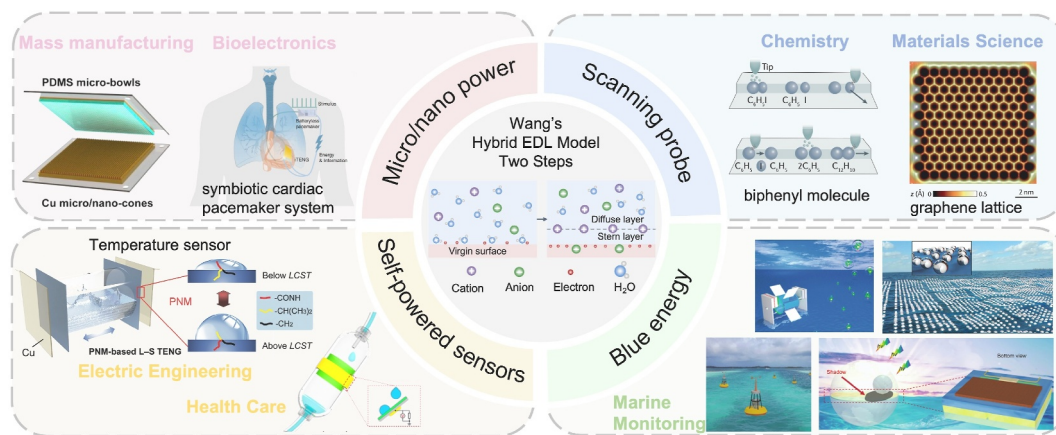


FIGURE 14 Principal applications of liquid–solid interface triboelectricity based on Wang's hybrid Electric Double Layer (EDL) two-step model and its related fields.

research, efforts could be organized into three critical areas: interface engineering, focusing on enhancing charge transfer and reducing energy losses; material discovery, aimed at identifying new materials with superior properties; and theoretical modeling, which will help deepen our understanding of charge transfer mechanisms and provide predictive insights for system optimization.

5.2.1 | Interface engineering

Future research could focus on interface engineering to improve charge transfer efficiency and reduce energy loss. This includes exploring surface modification techniques such as surface functionalization, nanostructuring, and surface coatings, which can enhance the interaction at the liquid–solid interface. Additionally, optimizing the interface configuration and geometry can further improve charge generation and collection, thereby increasing the output performance of TENGs.

5.2.2 | Material discovery

Understanding and controlling the properties of materials at the liquid–solid interface is critical for improving the output performance of TENGs. Research efforts should focus on discovering new materials with enhanced triboelectric behavior, electrical conductivity, and mechanical flexibility. Furthermore, developing architected systems or hybrid materials could significantly improve the stability and durability of TENG devices.

5.2.3 | Theoretical modeling and simulations

Despite significant progress in the study of solid–liquid interface triboelectricity, many challenges remain in

understanding the underlying mechanisms. Future studies should delve into charge transfer processes, interface phenomena, and energy conversion mechanisms at the molecular and atomic levels. Advanced theoretical modeling, computational simulations, and experimental techniques will be essential for revealing the complex dynamics during CE at the liquid–solid interface.

ACKNOWLEDGMENTS

This research was partially supported by funding from the Australian Research Council (ARC) through the ARC Center of Excellence in Future Low-Energy Electronics Technologies (CE170100039), an Australian Government Global Innovation Linkage Program (GIL 73629), a National Key R & D Project from the Minister of Science and Technology of China (Grant No. 2016YFA0202704), the National Natural Science Foundation of China (Grant Nos. 62001031, 51702018, and 51432005), the China Postdoctoral Science Foundation (Grant No. 2019M660766), and the Fundamental Research Funds for the Central Universities of China (Grant No. E0E48957).

CONFLICT OF INTEREST STATEMENT

The authors declare no conflicts of interest.

DATA AVAILABILITY STATEMENT

Data sharing is not applicable to this article as no new data were created or analyzed in this study.

ORCID

Yahua He  <https://orcid.org/0000-0003-0674-808X>

Xiaolin Wang  <https://orcid.org/0000-0002-9001-8049>

REFERENCES

1. Hinchet R, Yoon H-J, RYU H, Kim M-K, Choi E-K, Kim D-S, Kim S-W. Transcutaneous ultrasound energy harvesting using capacitive triboelectric technology. *Science*. 2019; 365(6452):491-494.

2. Lin ZH, Cheng G, Lin L, Lee S, Wang ZL. Water–solid surface contact electrification and its use for harvesting liquid-wave energy. *Angew Chem Int Ed Engl.* 2013;52(48):12545-12549.
3. Rodrigues C, Nunes D, Clemente D, et al. Emerging triboelectric nanogenerators for ocean wave energy harvesting: state of the art and future perspectives. *Energy Environ Sci.* 2020;13(9):2657-2683.
4. Wang ZL. Triboelectric nanogenerators as new energy technology and self-powered sensors—Principles, problems and perspectives. *Faraday Discuss.* 2014;176:447-458.
5. Cheng T, Shao J, Wang ZL. Triboelectric nanogenerators. *Nat Rev Methods Primers.* 2023;3(1):39.
6. Zhai H, Ding S, Chen X, Wu Y, Wang ZL. Advances in solid–solid contacting triboelectric nanogenerator for ocean energy harvesting. *Mater Today.* 2023;65:166-188.
7. Cheng G, Zhang T, Fu X, et al. A comprehensive review of advancements and challenges from solid–solid to liquid–solid triboelectric nanogenerators. *Adv Mater Technol.* 2024;9(6):2301588.
8. Huang T, Long Y, Dong Z, et al. Ultralight, elastic, hybrid aerogel for flexible/wearable piezoresistive sensor and solid–solid/gas–solid coupled triboelectric nanogenerator. *Adv Sci.* 2022;9(34):2204519.
9. Chen Y, Pu X, Liu M, et al. Shape-adaptive, self-healable triboelectric nanogenerator with enhanced performances by soft solid–solid contact electrification. *ACS Nano.* 2019;13(8):8936-8945.
10. Chen H, Lu Q, Cao X, Wang N, Wang ZL. Natural polymers based triboelectric nanogenerator for harvesting biomechanical energy and monitoring human motion. *Nano Res.* 2022;15(3):2505-2511.
11. Adhikary P, Mahmud MP, Solaiman T, Wang ZL. Recent advances on biomechanical motion-driven triboelectric nanogenerators for drug delivery. *Nano Today.* 2022;45:101513.
12. Zou Y, Raveendran V, Chen J. Wearable triboelectric nanogenerators for biomechanical energy harvesting. *Nano Energy.* 2020;77:105303.
13. Cho S, Yun Y, Jang S, et al. Universal biomechanical energy harvesting from joint movements using a direction-switchable triboelectric nanogenerator. *Nano Energy.* 2020;71:104584.
14. Liu Z, Nie J, Miao B, et al. Self-powered intracellular drug delivery by a biomechanical energy-driven triboelectric nanogenerator. *Adv Mater.* 2019;31(12):1807795.
15. He J, Qian S, Niu X, et al. Piezoelectric-enhanced triboelectric nanogenerator fabric for biomechanical energy harvesting. *Nano Energy.* 2019;64:103933.
16. Qin Y, Fu X, Lin Y, Wang Z, Cao J, Zhang C. Self-powered Internet of Things sensing node based on triboelectric nanogenerator for sustainable environmental monitoring. *Nano Res.* 2023;16(9):11878-11884.
17. Zhou Z, Li X, Wu Y, et al. Wireless self-powered sensor networks driven by triboelectric nanogenerator for in-situ real time survey of environmental monitoring. *Nano Energy.* 2018;53:501-507.
18. Chang A, Uy C, Xiao X, Chen J. Self-powered environmental monitoring via a triboelectric nanogenerator. *Nano Energy.* 2022;98:107282.
19. Seung W, Gupta MK, Lee KY, et al. Nanopatterned textile-based wearable triboelectric nanogenerator. *ACS Nano.* 2015;9(4):3501-3509.
20. Mathew AA, Chandrasekhar A, Vivekanandan S. A review on real-time implantable and wearable health monitoring sensors based on triboelectric nanogenerator approach. *Nano Energy.* 2021;80:105566.
21. Liu Z, Li H, Shi B, Fan Y, Wang ZL, Li Z. Wearable and implantable triboelectric nanogenerators. *Adv Funct Mater.* 2019;29(20):1808820.
22. Wang H, Han M, Song Y, Zhang H. Design, manufacturing and applications of wearable triboelectric nanogenerators. *Nano Energy.* 2021;81:105627.
23. Zhang B, Tang Y, Dai R, et al. Breath-based human–machine interaction system using triboelectric nanogenerator. *Nano Energy.* 2019;64:103953.
24. Pu X, An S, Tang Q, Guo H, Hu C. Wearable triboelectric sensors for biomedical monitoring and human–machine interface. *iScience.* 2021;24(1):102027.
25. Doganay D, Cicek MO, Durukan MB, et al. Fabric based wearable triboelectric nanogenerators for human machine interface. *Nano Energy.* 2021;89:106412.
26. Ding W, Wang AC, Wu C, Guo H, Wang ZL. Human–machine interfacing enabled by triboelectric nanogenerators and tribotronics. *Adv Mater Technol.* 2019;4(1):1800487.
27. Wang Y, Gao S, Xu W, Wang Z. Nanogenerators with superwetting surfaces for harvesting water/liquid energy. *Adv Funct Mater.* 2020;30(26):1908252.
28. Wang P, Zhang S, Zhang L, Wang L, Xue H, Wang ZL. Non-contact and liquid–liquid interfacing triboelectric nanogenerator for self-powered water/liquid level sensing. *Nano Energy.* 2020;72:104703.
29. Li X, Tao J, Wang X, Zhu J, Pan C, Wang ZL. Networks of high performance triboelectric nanogenerators based on liquid–solid interface contact electrification for harvesting low-frequency blue energy. *Adv Energy Mater.* 2018;8(21).
30. Tao X, Nie J, Li S, et al. Effect of photo-excitation on contact electrification at liquid–solid interface. *ACS Nano.* 2021;15(6):10609-10617.
31. Zhao XJ, Kuang SY, Wang ZL, Zhu G. Highly adaptive solid–liquid interfacing triboelectric nanogenerator for harvesting diverse water wave energy. *ACS Nano.* 2018;12(5):4280-4285.
32. Tang W, Chen BD, Wang ZL. Recent progress in power generation from water/liquid droplet interaction with solid surfaces. *Adv Funct Mater.* 2019;29(41).
33. Zhao XJ, Kuang SY, Wang ZL, Zhu G. Highly adaptive solid–liquid interfacing triboelectric nanogenerator for harvesting diverse water wave energy. *ACS Nano.* 2018;12(5):4280-4285.
34. Xu W, Yang J, Liu S, et al. An instantaneous discharging liquid–solid triboelectric nanogenerator (IDLS-TENG) with boosted peak power output. *Nano Energy.* 2021;86:106093.
35. Pan L, Wang J, Wang P, et al. Liquid-FEP-based U-tube triboelectric nanogenerator for harvesting water-wave energy. *Nano Res.* 2018;11(8):4062-4073.
36. Nie J, Ren Z, Xu L, et al. Probing contact-electrification-induced electron and ion transfers at a liquid–solid interface. *Adv Mater.* 2020;32(2):e1905696.
37. Tang Z, Lin S, Wang ZL. Quantifying contact-electrification induced charge transfer on a liquid droplet after contacting with a liquid or solid. *Adv Mater.* 2021;33(42):e2102886.
38. Zhao J, Wang D, Zhang F, et al. Self-powered, long-durable, and highly selective oil–solid triboelectric nanogenerator for

- energy harvesting and intelligent monitoring. *Nano-Micro Lett.* 2022;14(1):160.
39. Jiang P, Zhang L, Guo H, et al. Signal output of triboelectric nanogenerator at oil-water-solid multiphase interfaces and its application for dual-signal chemical sensing. *Adv Mater.* 2019;31(39):e1902793.
 40. You J, Shao J, He Y, et al. High-electrification performance and mechanism of a water-solid mode triboelectric nanogenerator. *ACS Nano.* 2021;15(5):8706-8714.
 41. Zou H, Zhang Y, Guo L, et al. Quantifying the triboelectric series. *Nat Commun.* 2019;10(1):1427.
 42. Zou H, Guo L, Xue H, et al. Quantifying and understanding the triboelectric series of inorganic non-metallic materials. *Nat Commun.* 2020;11(1):2093.
 43. Lin S, Xu L, Chi Wang A, Wang ZL. Quantifying electron-transfer in liquid-solid contact electrification and the formation of electric double-layer. *Nat Commun.* 2020; 11(1):399.
 44. Sun Y, Zheng Y, Wang R, et al. 3D micro-nanostructure based waterproof triboelectric nanogenerator as an outdoor adventure power source. *Nano Energy.* 2022;100:107506.
 45. Sun B, Xu D, Wang Z, Zhan Y, Zhang K. Interfacial structure design for triboelectric nanogenerators. *Battery Energy.* 2022; 1(3):20220001.
 46. Park J, Lee Y, Ha M, Cho S, Ko H. Micro/nanostructured surfaces for self-powered and multifunctional electronic skins. *J Mater Chem B.* 2016;4(18):2999-3018.
 47. Lee KY, Chun J, Lee J-H, et al. Hydrophobic sponge structure-based triboelectric nanogenerator. *Adv Mater.* 2014;26(29): 5037-5042.
 48. Yu Y, Wang X. Chemical modification of polymer surfaces for advanced triboelectric nanogenerator development. *Extreme Mech Lett.* 2016;9:514-530.
 49. Liu Y, Mo J, Fu Q, et al. Enhancement of triboelectric charge density by chemical functionalization. *Adv Funct Mater.* 2020;30(50):2004714.
 50. Liu Y, Fu Q, Mo J, et al. Chemically tailored molecular surface modification of cellulose nanofibrils for manipulating the charge density of triboelectric nanogenerators. *Nano Energy.* 2021;89:106369.
 51. Ibrahim M, Jiang J, Wen Z, Sun X. Surface engineering for enhanced triboelectric nanogenerator. *Nanoenergy Adv.* 2021; 1(1):58-80.
 52. Mishra S, Supraja P, Haranath D, Kumar RR, Pola S. Effect of surface and contact points modification on the output performance of triboelectric nanogenerator. *Nano Energy.* 2022; 104:107964.
 53. Li HY, Su L, Kuang SY, Pan CF, Zhu G, Wang ZL. Significant enhancement of triboelectric charge density by fluorinated surface modification in nanoscale for converting mechanical energy. *Adv Funct Mater.* 2015;25(35):5691-5697.
 54. Wang ZL, Wang AC. On the origin of contact-electrification. *Mater Today.* 2019.
 55. Zheng M, Lin S, Zhu L, Tang Z, Wang ZL. Effects of temperature on the tribovoltaic effect at liquid-solid interfaces. *Adv Mater Interfac.* 2022;9(3):2101757.
 56. Wei K-Q, Sun D-J, Liu M-N, et al. Direct current nanogenerator based on tribovoltaic effect at WS₂ semiconductor interface. *ACS Appl Nano Mater.* 2024;7(2):1748-1756.
 57. Luo Q, Xiao K, Zhang J, Sun W. Direct-current triboelectric nanogenerators based on semiconductor structure. *ACS Appl Electron Mater.* 2022;4(9):4212-4230.
 58. Lin S, Chen X, Wang ZL. The tribovoltaic effect and electron transfer at a liquid-semiconductor interface. *Nano Energy.* 2020;76.
 59. Zheng M, Lin S, Zhu L, Tang Z, Wang ZL. Effects of temperature on the tribovoltaic effect at liquid-solid interfaces. *Adv Mater Interfac.* 2021;9(3).
 60. Le J, Fan Q, Perez-Martinez L, Cuesta A, Cheng J. Theoretical insight into the vibrational spectra of metal-water interfaces from density functional theory based molecular dynamics. *Phys Chem Chem Phys.* 2018;20(17):11554-11558.
 61. Zhang J, Lin S, Wang ZL. Electrostatic charges regulate chemiluminescence by electron transfer at the liquid-solid interface. *J Phys Chem B.* 2022;126(14):2754-2760.
 62. Nguyen QT, Vo CP, Nguyen TH, Kyoung KA. A direct-current triboelectric nanogenerator energy harvesting system based on water electrification for self-powered electronics. *Appl Sci.* 2022.
 63. Zhang C, Zhou L, Cheng P, et al. Surface charge density of triboelectric nanogenerators: theoretical boundary and optimization methodology. *Appl Mater Today.* 2020;18:100496.
 64. Pace G, Ansaldo A, Serri M, Lauciello S, Bonaccorso F. Electrode selection rules for enhancing the performance of triboelectric nanogenerators and the role of few-layers graphene. *Nano Energy.* 2020;76:104989.
 65. Lin S, Xu C, Xu L, Wang ZL. The overlapped electron-cloud model for electron transfer in contact electrification. *Adv Funct Mater.* 2020;30(11).
 66. Xu C, Wang AC, Zou H, et al. Raising the working temperature of a triboelectric nanogenerator by quenching down electron thermionic emission in contact-electrification. *Adv Mater.* 2018;30(38):1803968.
 67. Lin S, Chen X, Wang ZL. Contact electrification at the liquid-solid interface. *Chem Rev.* 2021.
 68. Moon JK, Jeong J, Lee D, Pak HK. Electrical power generation by mechanically modulating electrical double layers. *Nat Commun.* 2013;4:1487.
 69. Xu C, Zi Y, Wang AC, et al. On the electron-transfer mechanism in the contact-electrification effect. *Adv Mater.* 2018; 30(15):e1706790.
 70. Sriphan S, Vittayakorn N. Tribovoltaic effect: fundamental working mechanism and emerging applications. *Materials Today Nano.* 2023;22.
 71. Lin S, Lin Wang Z. The tribovoltaic effect. *Mater Today.* 2022.
 72. Wang Z, Zhang Z, Chen Y, et al. Achieving an ultrahigh direct-current voltage of 130 V by semiconductor heterojunction power generation based on the tribovoltaic effect. *Energy Environ Sci.* 2022;15(6):2366-2373.
 73. Huang Y, Liu D, Gao X, Zhu J, Zhang Y, Zhang M. Flexible liquid-based continuous direct-current tribovoltaic generators enable self-powered multi-modal sensing. *Adv Funct Mater.* 2022;33(1).
 74. Lu Y, Yan Y, Yu X, et al. Polarized water driven dynamic PN junction-based direct-current generator. *Research.* 2021.
 75. Yan Y, Zhou X, Feng S, et al. Direct current electricity generation from dynamic polarized water-semiconductor interface. *J Phys Chem C.* 2021;125(26):14180-14187.

76. Zhang Z, Jiang D, Zhao J, et al. Tribovoltaic effect on metal–semiconductor interface for direct-current low-impedance triboelectric nanogenerators. *Adv Energy Mater.* 2020;10(9).
77. Zheng M, Lin S, Xu L, Zhu L, Wang ZL. Scanning probing of the tribovoltaic effect at the sliding interface of two semiconductors. *Adv Mater.* 2020;32(21):e2000928.
78. Zheng M, Lin S, Tang Z, Feng Y, Wang ZL. Photovoltaic effect and tribovoltaic effect at liquid–semiconductor interface. *Nano Energy.* 2021;83.
79. Fan C, Shao J, Guo X, Willatzen M, Wang ZL. Field-circuit coupling model of triboelectric nanogenerators. *Mater Today Phys.* 2023;35:101124.
80. Shao J, Willatzen M, Wang ZL. Theoretical modeling of triboelectric nanogenerators (TENGs). *J Appl Phys.* 2020;128(11).
81. Shao J, Liu D, Willatzen M, Wang ZL. Three-dimensional modeling of alternating current triboelectric nanogenerator in the linear sliding mode. *Appl Phys Rev.* 2020;7(1).
82. Shao J, Jiang T, Tang W, Chen X, Xu L, Wang ZL. Structural figure-of-merits of triboelectric nanogenerators at powering loads. *Nano Energy.* 2018;51:688–697.
83. Niu S, Wang S, Lin L, et al. Theoretical study of contact-mode triboelectric nanogenerators as an effective power source. *Energy Environ Sci.* 2013;6(12).
84. Niu S, Liu Y, Wang S, et al. Theoretical investigation and structural optimization of single-electrode triboelectric nanogenerators. *Adv Funct Mater.* 2014;24(22):3332–3340.
85. Niu S, Liu Y, Chen X, et al. Theory of freestanding triboelectric-layer-based nanogenerators. *Nano Energy.* 2015;12:760–774.
86. Niu S, Wang ZL. Theoretical systems of triboelectric nanogenerators. *Nano Energy.* 2015;14:161–192.
87. Niu S, Liu Y, Wang S, et al. Theory of sliding-mode triboelectric nanogenerators. *Adv Mater.* 2013;25(43):6184–6193.
88. Jiang T, Chen X, Han CB, Tang W, Wang ZL. Theoretical study of rotary freestanding triboelectric nanogenerators. *Adv Funct Mater.* 2015;25(19):2928–2938.
89. Yu Z, Zhang Y, Willatzen M, Shao J, Wang ZL. Momentum transfer in triboelectric nanogenerators. *Adv Phys Resh.* 2023;2300115.
90. You J, Shao J, He Y, et al. Simulation model of a non-contact triboelectric nanogenerator based on electrostatic induction. *EcoMat.* 2023.
91. Xu W, Zheng H, Liu Y, et al. A droplet-based electricity generator with high instantaneous power density. *Nature.* 2020.
92. Wu H, Mendel N, van den Ende D, Zhou G, Mugele F. Energy harvesting from drops impacting onto charged surfaces. *Phys Rev Lett.* 2020;125(7):078301.
93. Wang D, Wang X-X, Jin ML, He P, Zhang S. Molecular level manipulation of charge density for solid–liquid TENG system by proton irradiation. *Nano Energy.* 2022;103:107819.
94. Kim Y, Lee D, Seong J, Bak B, Choi UH, Kim J. Ionic liquid-based molecular design for transparent, flexible, and fire-retardant triboelectric nanogenerator (TENG) for wearable energy solutions. *Nano Energy.* 2021;84:105925.
95. Jun Wu JC, Bi H, Zhang J, Cao Q. Liquid–solid contact electrification and its effect on the formation of electric double layer: an atomic-level investigation. *Nano Energy.* 2023.
96. Nan Y, Shao J, Willatzen M, Wang ZL. Understanding contact electrification at water/polymer interface. *Research.* 2022;2022:9861463.
97. Wang N, Zhang W, Li Z, et al. Dual-electric-polarity augmented cyanoethyl cellulose-based triboelectric nanogenerator with ultra-high triboelectric charge density and enhanced electrical output property at high humidity. *Nano Energy.* 2022;103:107748.
98. Wang D, Zhang D, Tang M, et al. Ethylene chlorotrifluoroethylene/hydrogel-based liquid–solid triboelectric nanogenerator driven self-powered MXene-based sensor system for marine environmental monitoring. *Nano Energy.* 2022;100:107509.
99. Singh S, Yadav P, Gupta MK, et al. Gigantic stimulation in response by solar irradiation in self-healable and self-powered LPG sensor based on triboelectric nanogenerator: experimental and DFT computational study. *Sensor Actuator B Chem.* 2022;359:131573.
100. Yang H, He J, Yan J, et al. Highly sensitive self-powered humidity sensor based on a TaS₂/Cu₂S heterostructure driven by a triboelectric nanogenerator. *ACS Appl Mater Interfaces.* 2023;15(27):33077–33086.
101. Shin S-H, Bae YE, Moon HK, et al. Formation of triboelectric series via atomic-level surface functionalization for triboelectric energy harvesting. *ACS Nano.* 2017;11(6):6131–6138.
102. Lee JW, Jung S, Jo J, et al. Sustainable highly charged C 60-functionalized polyimide in a non-contact mode triboelectric nanogenerator. *Energy Environ Sci.* 2021;14(2):1004–1015.
103. Khandelwal G, Maria Joseph Raj NP, Kim SJ. Materials beyond conventional triboelectric series for fabrication and applications of triboelectric nanogenerators. *Adv Energy Mater.* 2021;11(33):2101170.
104. Kwon YH, Shin S-H, Kim Y-H, Jung J-Y, Lee MH, Nah J. Triboelectric contact surface charge modulation and piezoelectric charge inducement using polarized composite thin film for performance enhancement of triboelectric generators. *Nano Energy.* 2016;25:225–231.
105. Zhang J-H, Zhang Y, Sun N, et al. Enhancing output performance of triboelectric nanogenerator via large polarization difference effect. *Nano Energy.* 2021;84:105892.
106. Wu H, He W, Shan C, et al. Achieving remarkable charge density via self-polarization of polar high-k material in a charge-excitation triboelectric nanogenerator. *Adv Mater.* 2022;34(13):2109918.
107. Wang J, Wu H, Wang Z, et al. An ultrafast self-polarization effect in barium titanate filled poly (vinylidene fluoride) composite film enabled by self-charge excitation triboelectric nanogenerator. *Adv Funct Mater.* 2022;32(35):2204322.
108. Guo X, Shao J, Willatzen M, Wang X, Wang ZL. Quantifying output power and dynamic charge distribution in sliding mode freestanding triboelectric nanogenerator. *Adv Phys Res.* 2023;2(2):2200039.
109. Shin E, Ko J-H, Lyeo H-K, Kim Y-H. First theoretical triboelectric series. *APS March Meeting Abstracts.* 2022.
110. Liu T, Mo W, Zou X, et al. Liquid–solid triboelectric probes for real-time monitoring of sucrose fluid status. *Adv Funct Mater.* 2023;33(45):2304321.

111. Liu J, Wen Z, Lei H, Gao Z, Sun X. A liquid–solid interface-based triboelectric tactile sensor with ultrahigh sensitivity of 21.48 kPa^{-1} . *Nano-Micro Lett.* 2022;14(1):88.
112. Zeng Q, Wu Y, Tang Q, et al. A high-efficient breeze energy harvester utilizing a full-packaged triboelectric nanogenerator based on flow-induced vibration. *Nano Energy.* 2020;70:104524.
113. Ren Z, Wang Z, Wang F, Li S, Wang ZL. Vibration behavior and excitation mechanism of ultra-stretchable triboelectric nanogenerator for wind energy harvesting. *Extreme Mech Lett.* 2021;45:101285.
114. Kim Y, Yun J, Kim D. Robust and flexible triboelectric nanogenerator using non-Newtonian fluid characteristics towards smart traffic and human-motion detecting system. *Nano Energy.* 2022;98:107246.
115. Kim H, Zhou Q, Kim D, Oh I-K. Flow-induced snap-through triboelectric nanogenerator. *Nano Energy.* 2020;68:104379.
116. Cao LN, Xu Z, Wang ZL. Application of triboelectric nanogenerator in fluid dynamics sensing: past and future. *Nano-materials.* 2022;12(19):3261.
117. Tan D, Zhou J, Wang K, Zhang C, Li Z, Xu D. Wearable bistable triboelectric nanogenerator for harvesting torsional vibration energy from human motion. *Nano Energy.* 2023; 109:108315.
118. Zhou T, Zhang C, Han CB, Fan FR, Tang W, Wang ZL. Woven structured triboelectric nanogenerator for wearable devices. *ACS Appl Mater Interfaces.* 2014;6(16):14695-14701.
119. Xiao X, Chen G, Libanori A, Chen J. Wearable triboelectric nanogenerators for therapeutics. *Trends Chem.* 2021;3(4): 279-290.
120. Luo J, Gao W, Wang ZL. The triboelectric nanogenerator as an innovative technology toward intelligent sports. *Adv Mater.* 2021;33(17):2004178.
121. Li S, Wang J, Peng W, et al. Sustainable energy source for wearable electronics based on multilayer elastomeric triboelectric nanogenerators. *Adv Energy Mater.* 2017;7(13): 1602832.
122. Tang W, Han Y, Han CB, Gao CZ, Cao X, Wang ZL. Self-powered water splitting using flowing kinetic energy. *Adv Mater.* 2015;27(2):272-276.
123. Zou Y, Tan P, Shi B, et al. A bionic stretchable nanogenerator for underwater sensing and energy harvesting. *Nat Commun.* 2019;10(1):2695.
124. Zhang X-S, Han M-D, Meng B, Zhang H-X. High performance triboelectric nanogenerators based on large-scale mass-fabrication technologies. *Nano Energy.* 2015;11:304-322.
125. Zhang C, Bu T, Zhao J, Liu G, Yang H, Wang ZL. Tribotronics for active mechanosensation and self-powered microsystems. *Adv Funct Mater.* 2019;29(41):1808114.
126. Jiang Q, Wu C, Wang Z, et al. MXene electrochemical microsupercapacitor integrated with triboelectric nanogenerator as a wearable self-charging power unit. *Nano Energy.* 2018;45:266-272.
127. Liu H, Xu Y, Xiao Y, et al. Highly adaptive liquid–solid triboelectric nanogenerator-assisted self-powered water wave motion sensor. *ACS Appl Electron Mater.* 2022;4(8): 3870-3879.
128. Jiang L, Liu X, Lv J, et al. Fluid-based triboelectric nanogenerators: unveiling the prolific landscape of renewable energy harvesting and beyond. *Energy Environ Sci.* 2024; 17(11):3700-3738.
129. Cheng G, Lin Z-H, Du Z-I, Wang ZL. Simultaneously harvesting electrostatic and mechanical energies from flowing water by a hybridized triboelectric nanogenerator. *ACS Nano.* 2014;8(2):1932-1939.
130. Zhan T, Zou H, Zhang H, et al. Smart liquid-piston based triboelectric nanogenerator sensor for real-time monitoring of fluid status. *Nano Energy.* 2023;111:108419.
131. Chen J, Guo H, Zheng J, et al. Self-powered triboelectric micro liquid/gas flow sensor for microfluidics. *ACS Nano.* 2016;10(8):8104-8112.
132. Tian J, Chen X, Wang ZL. Environmental energy harvesting based on triboelectric nanogenerators. *Nanotechnology.* 2020; 31(24):242001.
133. Graham SA, Chandrarathna SC, Patnam H, Manchi P, Lee J-W, Yu JS. Harsh environment-tolerant and robust triboelectric nanogenerators for mechanical-energy harvesting, sensing, and energy storage in a smart home. *Nano Energy.* 2021;80:105547.
134. Chen H, Xing C, Li Y, Wang J, Xu Y. Triboelectric nanogenerators for a macro-scale blue energy harvesting and self-powered marine environmental monitoring system. *Sustain Energy Fuels.* 2020;4(3):1063-1077.
135. Yong S, Wang H, Lin Z, et al. Environmental self-adaptive wind energy harvesting technology for self-powered system by triboelectric-electromagnetic hybridized nanogenerator with dual-channel power management topology. *Adv Energy Mater.* 2022;12(43):2202469.
136. Pang Y, Cao Y, Derakhshani M, Fang Y, Wang ZL, Cao C. Hybrid energy-harvesting systems based on triboelectric nanogenerators. *Matter.* 2021;4(1):116-143.
137. Zhang J, Lin S, Zheng M, Wang ZL. Triboelectric nanogenerator as a probe for measuring the charge transfer between liquid and solid surfaces. *ACS Nano.* 2021;15(9):14830-14837.
138. Zhang J, Lin S, Wang ZL. Triboelectric nanogenerator array as a probe for in situ dynamic mapping of interface charge transfer at a liquid-solid contacting. *ACS Nano.* 2023;17(2): 1646-1652.
139. Zhou Q, Pan J, Deng S, Xia F, Kim T. Triboelectric nanogenerator-based sensor systems for chemical or biological detection. *Adv Mater.* 2021;33(35):2008276.
140. Zhao G, Zhang Y, Shi N, et al. Transparent and stretchable triboelectric nanogenerator for self-powered tactile sensing. *Nano Energy.* 2019;59:302-310.
141. Yang D, Ni Y, Kong X, et al. Self-healing and elastic triboelectric nanogenerators for muscle motion monitoring and photothermal treatment. *ACS Nano.* 2021;15(9):14653-14661.
142. Varghese H, Hakkeem HMA, Chauhan K, Thouti E, Pillai S, Chandran A. A high-performance flexible triboelectric nanogenerator based on cellulose acetate nanofibers and micropatterned PDMS films as mechanical energy harvester and self-powered vibrational sensor. *Nano Energy.* 2022;98: 107339.
143. Ferrie S, Le Brun AP, Krishnan G, Andersson GG, Darwish N, Ciampi S. Sliding silicon-based Schottky diodes: maximizing triboelectricity with surface chemistry. *Nano Energy.* 2022;93:106861.

144. Chen S, Wang N, Ma L, et al. Triboelectric nanogenerator for sustainable wastewater treatment via a self-powered electrochemical process. *Adv Energy Mater.* 2016;6(8).
145. Nie J, Ren Z, Shao J, et al. Self-powered microfluidic transport system based on triboelectric nanogenerator and electrowetting technique. *ACS Nano.* 2018;12(2):1491-1499.
146. Zheng L, Wu Y, Chen X, et al. Self-powered electrostatic actuation systems for manipulating the movement of both microfluid and solid objects by using triboelectric nanogenerator. *Adv Funct Mater.* 2017;27(16):1606408.
147. Shi Q, He T, Lee C. More than energy harvesting—Combining triboelectric nanogenerator and flexible electronics technology for enabling novel micro-/nano-systems. *Nano Energy.* 2019;57:851-871.
148. Ikram M, Mahmud MP. Advanced triboelectric nano generator-driven drug delivery systems for targeted therapies. *Drug Deliv Transl Res.* 2023;13(1):54-78.
149. Zheng L, Dong S, Nie J, et al. Dual-stimulus smart actuator and robot hand based on a vapor-responsive PDMS film and triboelectric nanogenerator. *ACS Appl Mater Interfaces.* 2019;11(45):42504-42511.
150. Zhao C, Cui X, Wu Y, Li Z. Recent progress of nanogenerators acting as self-powered drug delivery devices. *Adv Sustain Syst.* 2021;5(4):2000268.
151. Xu C, Song Y, Han M, Zhang H. Portable and wearable self-powered systems based on emerging energy harvesting technology. *Microsyst Nanoeng.* 2021;7(1):25.
152. Wu Z. Triboelectric nanogenerator for human-machine interfacing. In: *Handbook of Triboelectric Nanogenerators.* Springer; 2023:1-29.
153. Hamid HA, Celik-Butler Z. Design and optimization of a MEMS triboelectric energy harvester for nano-sensor applications. In: *2019 IEEE Sensors Applications Symposium (SAS);* 2019.
154. Dai Z, Feng K, Wang M, et al. Optimization of bidirectional bending sensor as flexible ternary terminal for high-capacity human-machine interaction. *Nano Energy.* 2022;97:107173.
155. Wang S, Xu P, Liu J, et al. Underwater triboelectric nanogenerator. *Nano Energy.* 2023;118:109018.

AUTHOR BIOGRAPHIES



Jing You received her Ph.D. degree from the University of Wollongong (UOW) in 2024 under the supervision of Prof. Khay See and Prof. Xiaolin Wang. Currently, she is a postdoctoral fellow at the school of Chemical Engineering, The University of New South Wales. Her research

interests include contact electrification, physical mechanisms of triboelectric nanogenerators, liquid metals, modeling, and simulation of the dynamic physical system.



Khay Wai See is a principal research fellow (Associate Professor) at the Australian Institute of Innovative Materials at the University of Wollongong, Australia.

He also currently holds the Interim Assistance Director for ISEM/EIS. With experience in both the industry and academia, he has worked extensively in superconductor applications for power utilities and large-scale battery energy storage. His key achievement is developing an advanced battery management system for lithium-ion batteries used in electric vehicles and renewable energy storage. His work bridges the gap between academic research and practical industry solutions.



Xiaolin Wang is the Director of Institute for Superconducting and Electronic Materials at the University of Wollongong and theme leader of the Australian Research Council Center of Excellence for Future Low Energy

Electronic technologies. He received his Ph.D. from the University of Wollongong, Australia. His main research interests cover superconductors, spintronic materials, topological insulators, quantum transport, liquid metals, interface triboelectricity, design of new materials, and physical properties. He proposed a new class of materials, coined as spin gapless materials which bridge the zero gap material and half metal and offer a new platform for high-performance spintronics and quantum anomalous Hall effect.

How to cite this article: You J, Shao J, He Y, et al. Interface triboelectricity. *EcoEnergy.* 2024;1-26. <https://doi.org/10.1002/ece2.78>